Passive Imaging & Monitoring in Wave Physics

New techniques in seismic tomography and joint inversion

Huajian Yao

University of Science and Technology of China (USTC)

with Hongjian Fang, Chuanming Liu, Shaoqian Hu, Haijiang Zhang, Hsin-Ying Yang (USTC), Rob van der Hilst (MIT), Cliff Thurber (UW Madison), Yehuda Ben-Zion (USC)

2019.9.16 Cargèse

Outline

1. Joint body & surface wave traveltime tomography for 3-D Vp, Vs, and Vp/Vs models: methodology and application to NE Tibet
2. Direct inversion of 3-D azimuthal and radial anisotropy from surface wave traveltime data: methodology and application to SE Tibet

classic datasets + improved techniques
→ reliable and useful models

Differences in tomographic models from different datasets
……but we only have one true model!

SE Tibet

Vs model from ambient noise + receiver functions

Vp model from local + teleseismic travel times

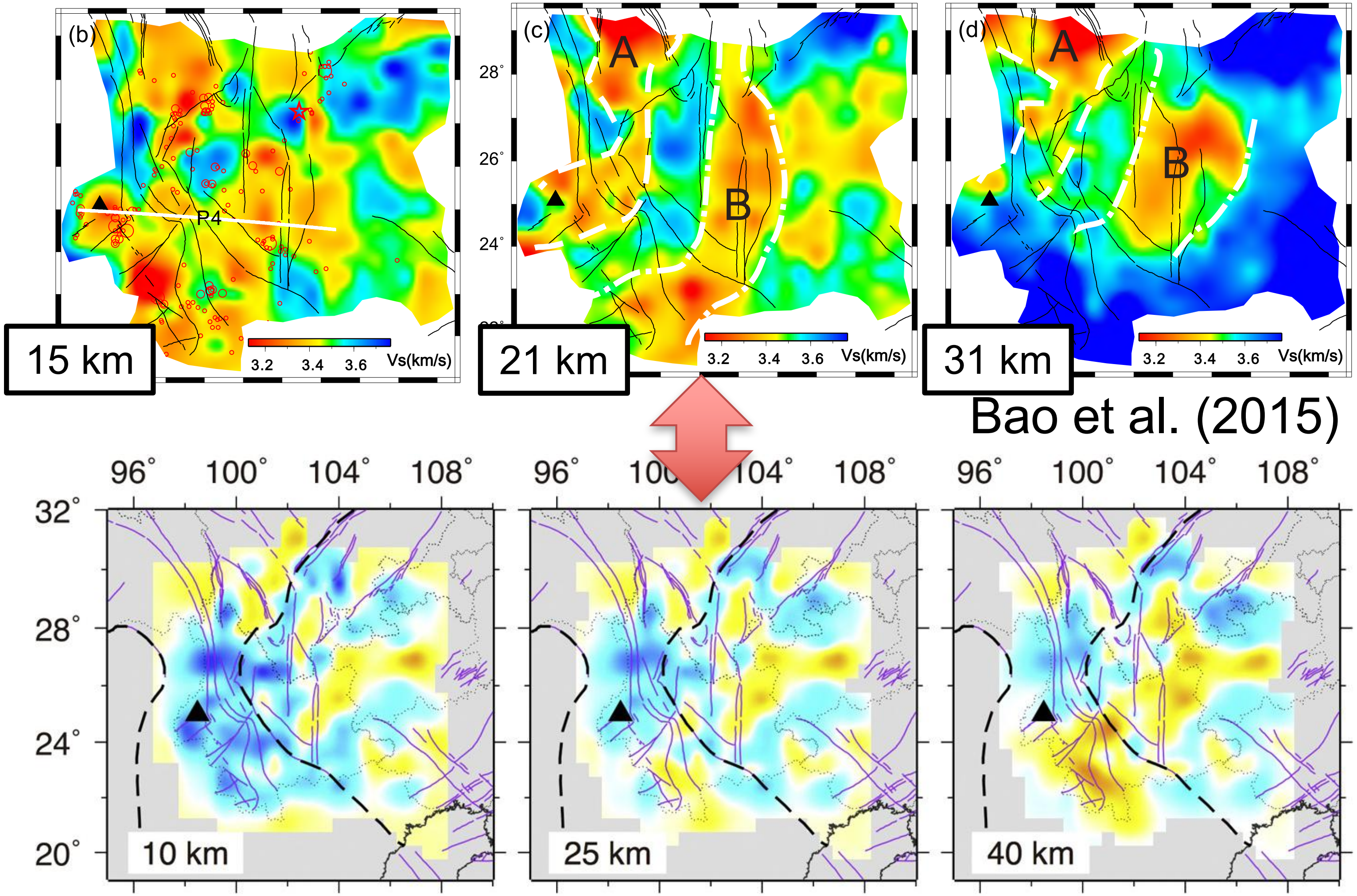

Bao et al. (2015)

Huang et al. (2015)

Different data: different constraints on the model
Joint seismic inversion: quest for the true model

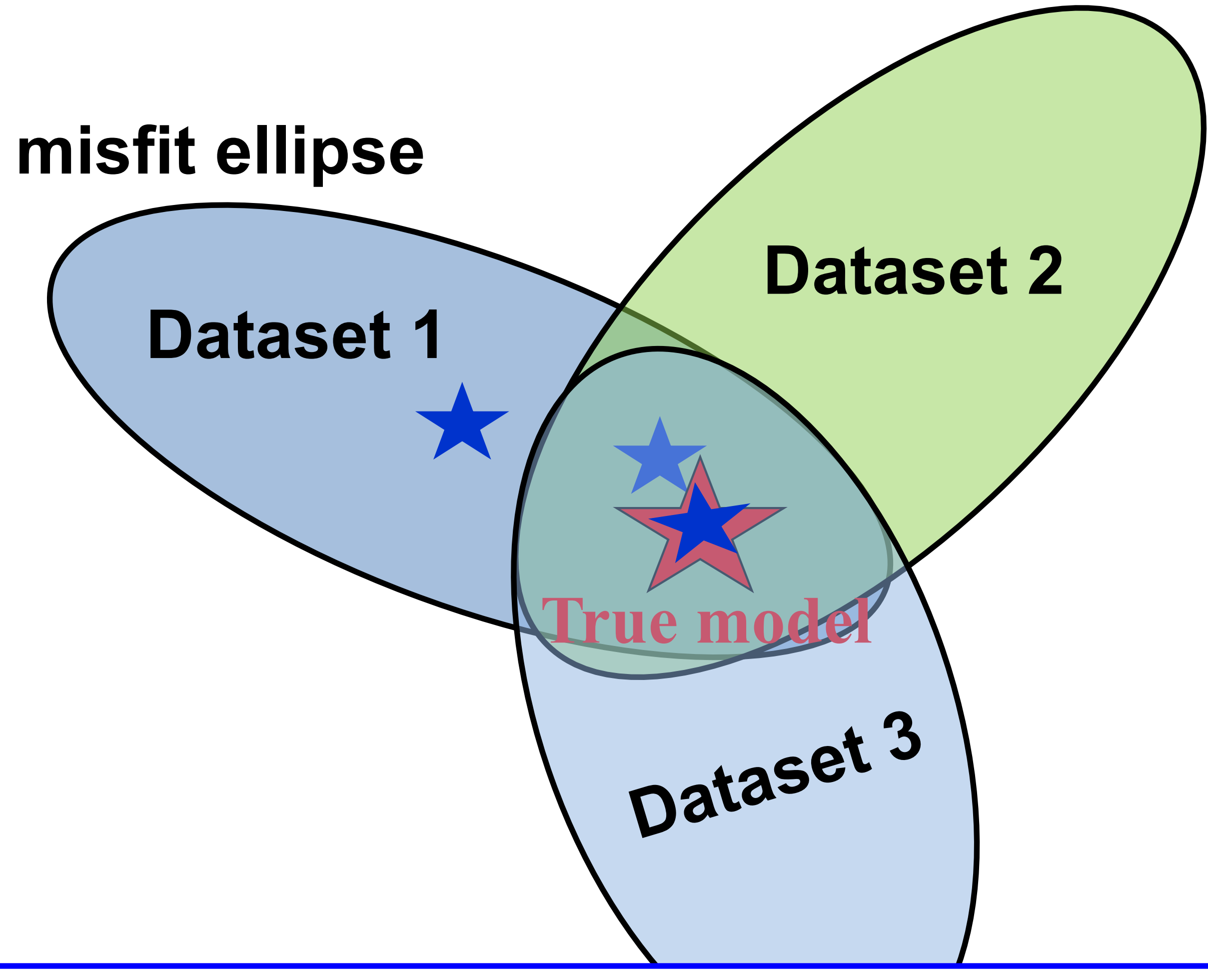

Joint inversion: avoid non-uniqueness of inversion using single dataset and get more reliable models

Why joint inversion using body wave + surface wave traveltimes?

Complementary strengths

- 1. Different depth and horizontal sensitivities

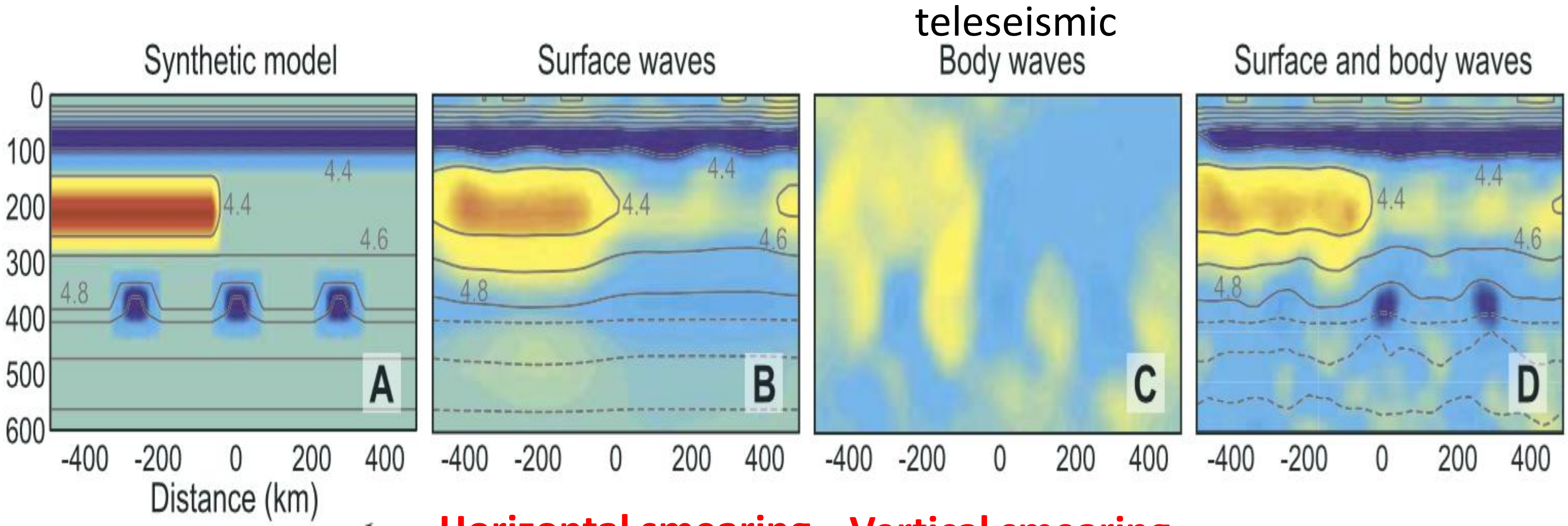

Horizontal smearing   Vertical smearing

West et al. (2004, GRL)

Why joint inversion using body wave + surface wave traveltimes?

- 2. Different model parameter sensitivity

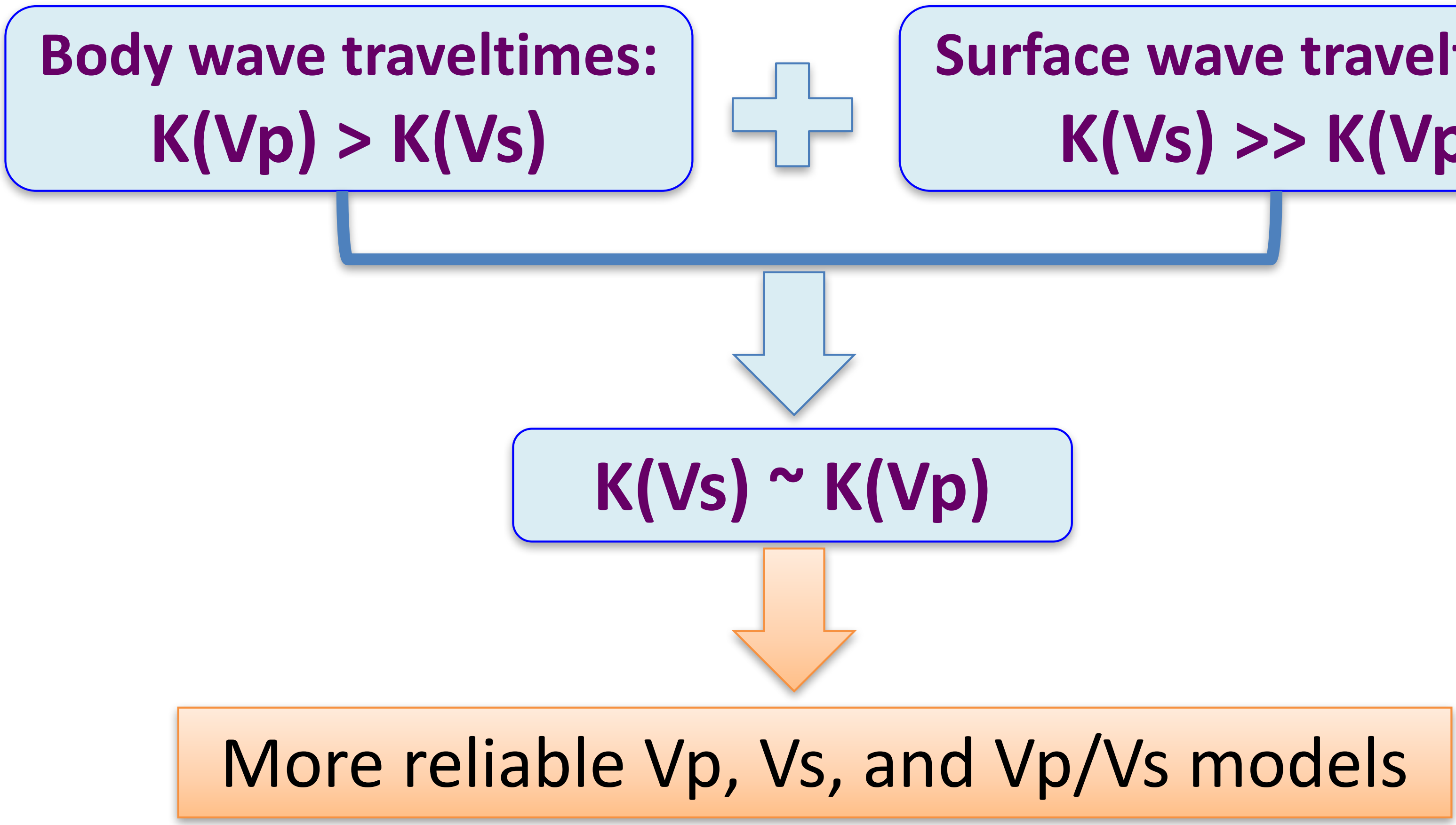

Background: surface wave tomography

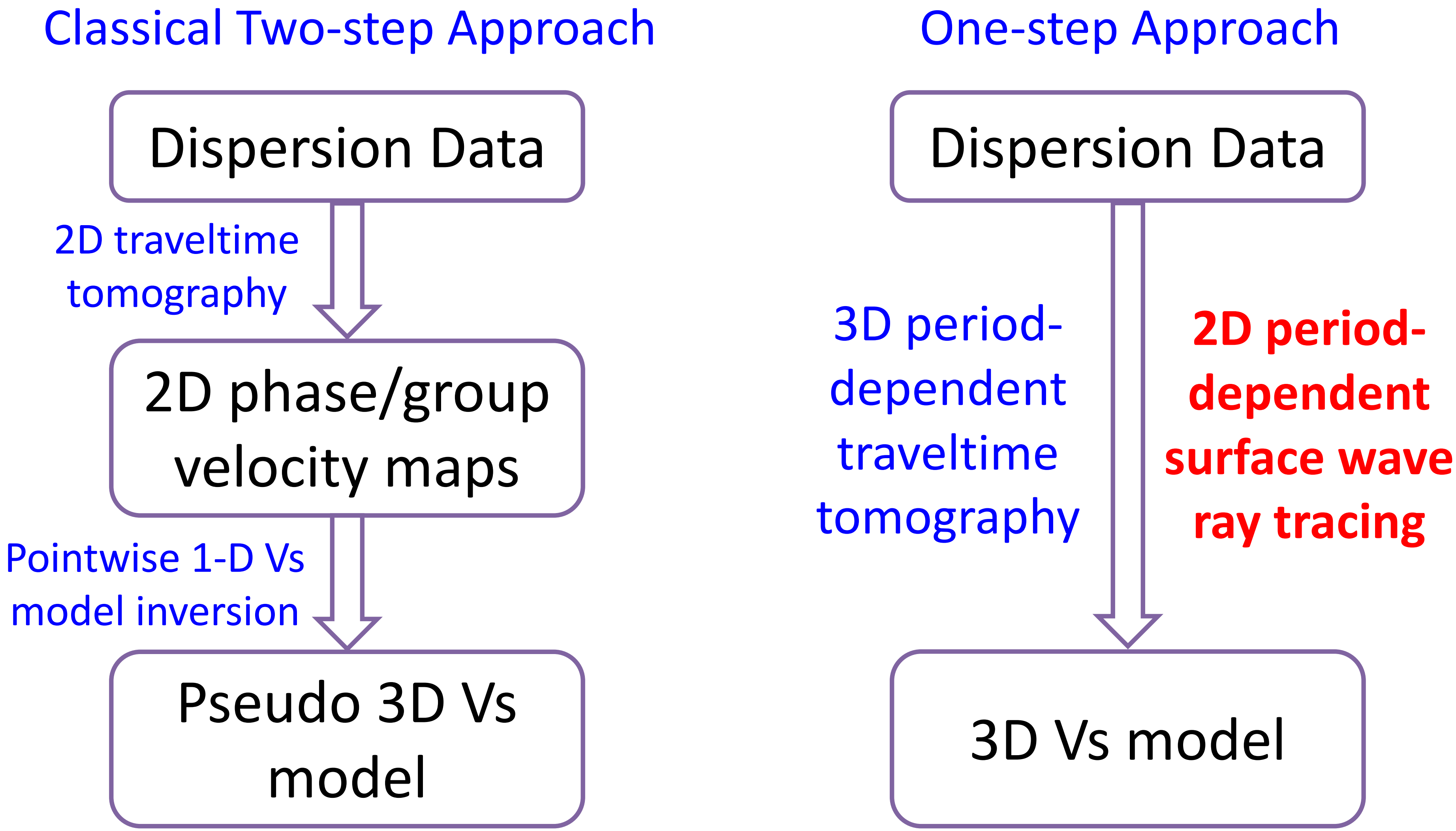

Fang, Yao, Zhang et al. (2015, GJI)

Direct inversion of 3-D Vs model from dispersion data with period dependent ray tracing

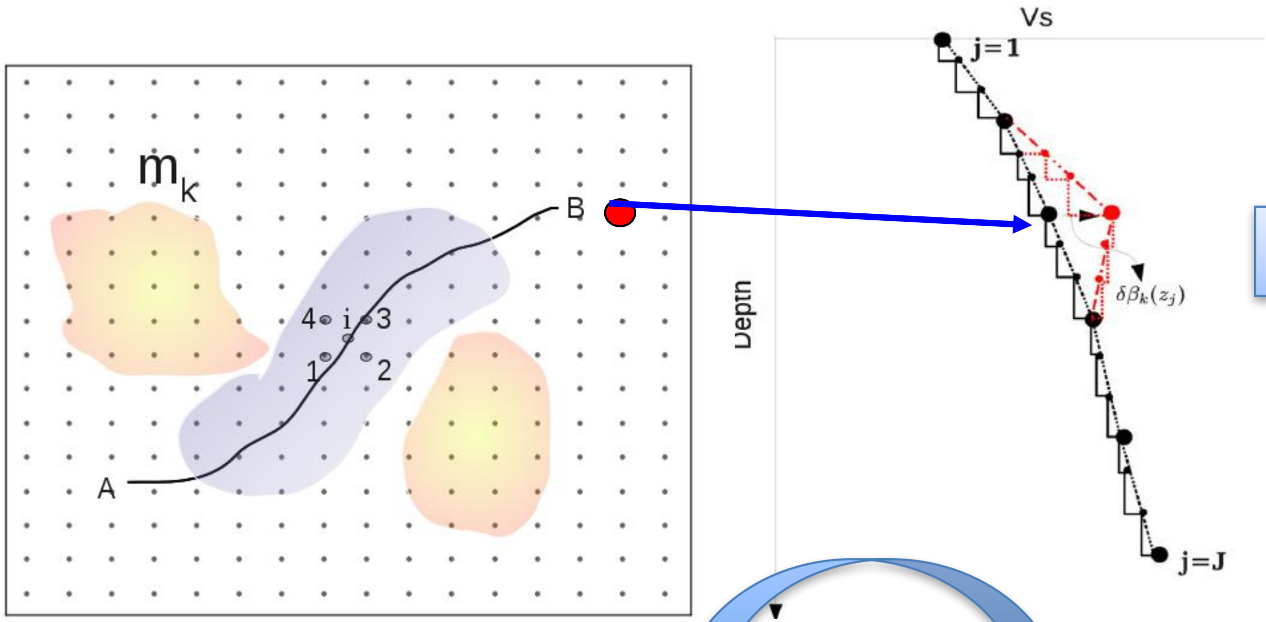

Update 3D model

Compute 2D Phase V

Update period-dependent ray paths & sensitivity matrix

$$\delta t(\omega) = \int K_s \delta C(\omega) ds$$

$$\delta C(\omega) = \int K_d \delta \beta dz$$

$$\delta t(\omega) = \int \mathbf{K} \delta \beta dv \Rightarrow \mathbf{Gm} = \mathbf{d}$$

Fang, Yao,Zhang et al. (2015, GJI)

code available at https://github.com/HongjianFang/DSurfTomo

Applications of DSurfTomo

1. Regional scale (a few hundred to thousand km→ crustal structure): Tibetan plateau, SW Tibet, SE China and Taiwan Straight, eastern China …

2. Local scale (~ ten to hundred km→shallow crust): Tanlu fault zone, Hefei City, Jinan City, Taipei Basin, Binchuan Basin in SW China, ….

3. Exploration scale (several km→near surface): shale gas production field, gas storage place, ….

Joint body & surface wave traveltime tomography for 3-D Vp and Vs models

Body wave
Traveltime tomo

$$\begin{bmatrix} \mathbf{G}_H^{T_p} & \mathbf{G}_{Vp}^{T_p} & \mathbf{0} \\ \mathbf{G}_H^{T_s} & \mathbf{0} & \mathbf{G}_{Vs}^{T_s} \end{bmatrix} \begin{bmatrix} \Delta\mathbf{H} \\ \Delta\mathbf{m}_p \\ \Delta\mathbf{m}_s \end{bmatrix} = \begin{bmatrix} \mathbf{d}^{T_p} \\ \mathbf{d}^{T_s} \end{bmatrix}$$

Direct Surface wave
Traveltime tomo

$$\begin{bmatrix} \mathbf{G}_{V_p}^{SW} & \mathbf{G}_{V_s}^{SW} \end{bmatrix} \begin{bmatrix} \Delta\mathbf{m}_p \\ \Delta\mathbf{m}_s \end{bmatrix} = \mathbf{d}^{SW}$$

period-dependent SW ray tracing
(Fang, Yao, Zhang et al. 2015, GJI.)

Joint body &
surface waves
tomo

$$\begin{bmatrix} \mathbf{G}_H^{T_p} & \mathbf{G}_{Vp}^{T_p} & \mathbf{0} \\ \mathbf{G}_H^{T_s} & \mathbf{0} & \mathbf{G}_{Vs}^{T_s} \\ \mathbf{0} & \alpha\mathbf{G}_{V_p}^{SW} & \alpha\mathbf{G}{V_s}^{SW} \end{bmatrix} \begin{bmatrix} \Delta\mathbf{H} \\ \Delta\mathbf{m}_p \\ \Delta\mathbf{m}_s \end{bmatrix} = \begin{bmatrix} \mathbf{d}^{T_p} \\ \mathbf{d}^{T_s} \\ \alpha\mathbf{d}^{SW} \end{bmatrix}$$

(Fang, Zhang, Yao et al., JGR 2016)

Joint body & surface wave traveltime tomography for 3-D Vp and Vs models

$$\begin{bmatrix} \mathbf{G}_H^{T_p} & \mathbf{G}_{V_p}^{T_p} & \mathbf{0} \\ \mathbf{G}_H^{T_s} & \mathbf{0} & \mathbf{G}_{V_s}^{T_s} \\ \mathbf{0} & \mu(\mathbf{G}_{V_p}^{SW} + R_\rho \mathbf{G}_\rho^{SW}) & \mu \mathbf{G}_{V_s}^{SW} \\ \mathbf{0} & \lambda_1 \mathbf{L} & \mathbf{0} \\ \mathbf{0} & \mathbf{0} & \lambda_2 \mathbf{L} \\ \mathbf{0} & \lambda_3 \mathbf{I} & -\lambda_3 \kappa \mathbf{I} \end{bmatrix} \begin{bmatrix} \Delta \mathbf{H} \\ \Delta \mathbf{m}_p \\ \Delta \mathbf{m}_s \end{bmatrix} = \begin{bmatrix} \mathbf{d}^{T_p} \\ \mathbf{d}^{T_s} \\ \mu \mathbf{d}^{SW} \\ \mathbf{0} \\ \mathbf{0} \\ \lambda_3 \kappa \mathbf{m}_s - \lambda_3 \mathbf{m}_p \end{bmatrix}$$

λ_1, λ_2: 3-D spatial smoothing

λ_3, κ: Vp/Vs ratio prior constraints

$$(\mathbf{m}_p + \Delta \mathbf{m}_p) = \kappa(\mathbf{m}_s + \Delta \mathbf{m}_s)$$

(Fang, Zhang, Yao et al., JGR 2016)

Joint Inversion for 3D Vp/Vs ratio

Fang, Yao, Zhang et al. (GJI, 2019)

$$\begin{bmatrix} \mathbf{G}_H^{T_p} & \mathbf{G}_{V_p}^{T_p} & \mathbf{0} \\ \mathbf{G}_H^{T_s} & \mathbf{0} & \mathbf{G}_{V_s}^{T_s} \\ \mathbf{0} & \mu\mathbf{G}_{V_p}^{SW} & \mu\mathbf{G}_{V_s}^{SW} \end{bmatrix} \begin{bmatrix} \Delta\mathbf{H} \\ \Delta\mathbf{V}_p \\ \Delta\mathbf{V}_s \end{bmatrix} = \begin{bmatrix} \mathbf{d}^{T_p} \\ \mathbf{d}^{T_s} \\ \mu\mathbf{d}^{SW} \end{bmatrix}$$

$$\kappa = \frac{Vp}{Vs} \quad \Rightarrow \quad \Delta\mathbf{V_s} = \frac{\mathbf{V_s}}{\mathbf{V_p}}\Delta\mathbf{V_p} - \frac{\mathbf{Vs^2}}{\mathbf{Vp}}\Delta\kappa$$

$$\Rightarrow \begin{bmatrix} \mathbf{G}_H^{T_p} & \mathbf{G}_{V_p}^{T_p} & \mathbf{0} \\ \mathbf{G}_H^{T_s} & \mathbf{G}_{V_s}^{T_s}\frac{\mathbf{V_s}}{\mathbf{V_p}} & -\mathbf{G}_{V_s}^{T_s}\frac{\mathbf{V_s^2}}{\mathbf{V_p}} \\ \mathbf{0} & \mu(\mathbf{G}_{V_p}^{SW} + \mathbf{G}_{V_s}^{SW}\frac{\mathbf{V_s}}{\mathbf{V_p}}) & -\mu\mathbf{G}_{V_s}^{SW}\frac{\mathbf{V_s}^2}{\mathbf{V_p}} \end{bmatrix} \begin{bmatrix} \Delta\mathbf{H} \\ \Delta\mathbf{V}_p \\ \Delta\kappa \end{bmatrix} = \begin{bmatrix} \mathbf{d}^{T_p} \\ \mathbf{d}^{T_s} \\ \mu\mathbf{d}^{SW} \end{bmatrix}$$

Add smoothing and damping directly to Vp/Vs to stabilize the inversion of 3-D Vp/Vs → lithology, partial melting?

Application to NE Tibetan Plateau

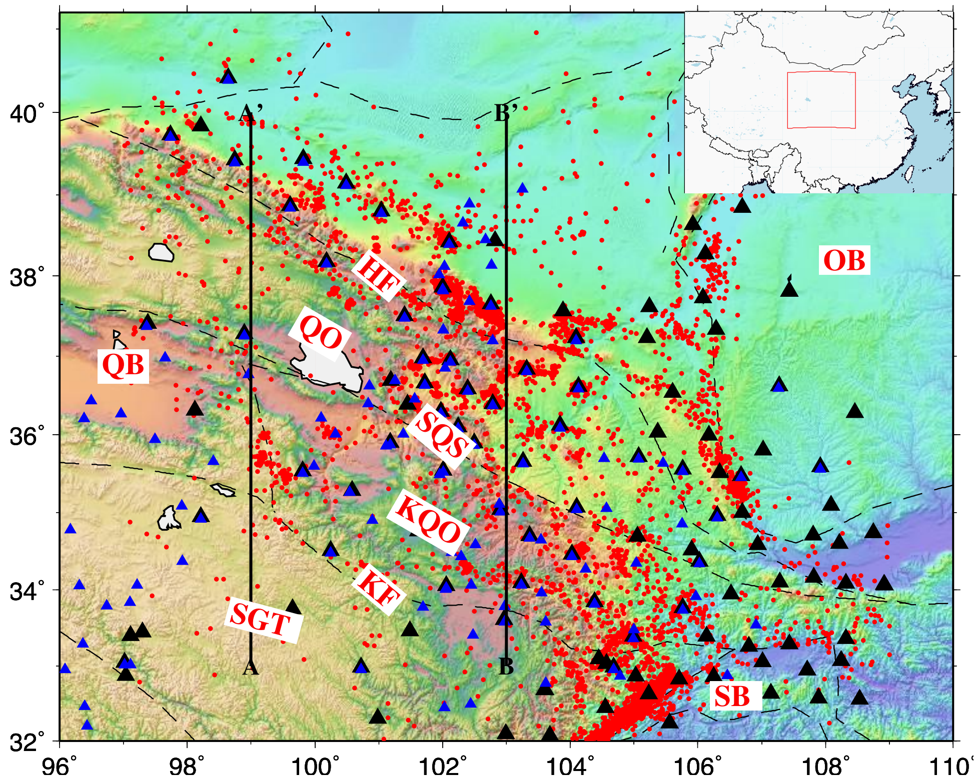

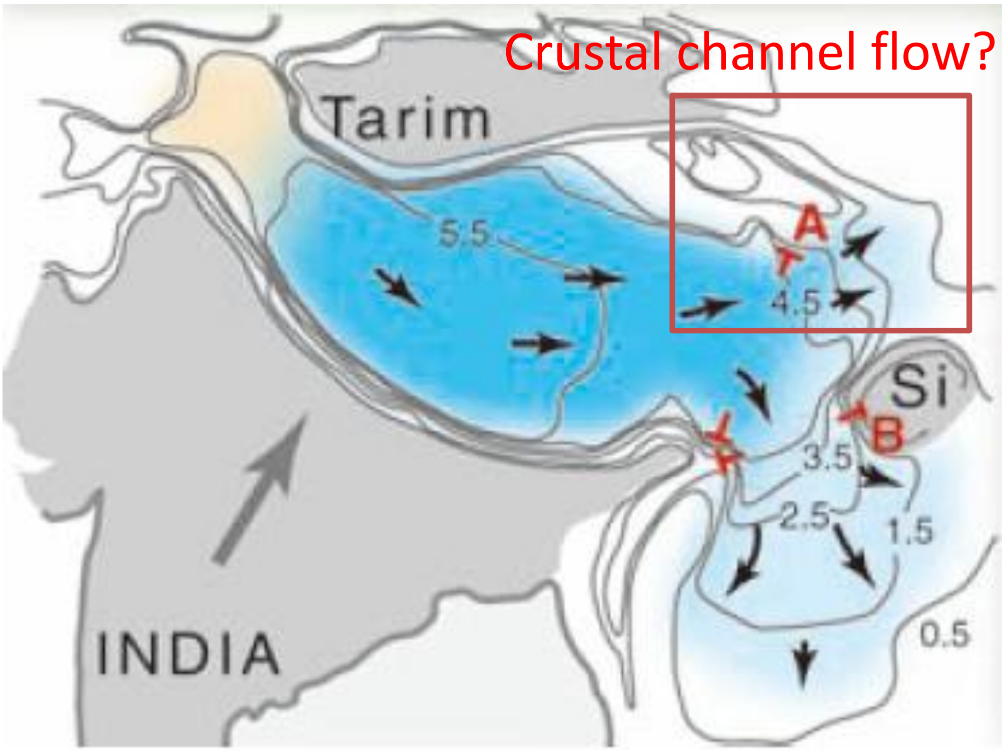

Royden et al. (2008)

Body wave traveltime data: P picks: ~ 300,000 S picks: ~ 290,000 (from Shunping Pei)

Surface wave traveltime data: Rayleigh wave phase velocity dispersion: ~ 51,000 (10 to 41 s) (from Hongyi Li)

Previous noise tomography results

prominent low-velocity zone in the middle crust of Qiangtang and Songpan-Ganze Terranes; no clear evidence of northeastward crustal flow to the Qilian Orogen

0-20 km

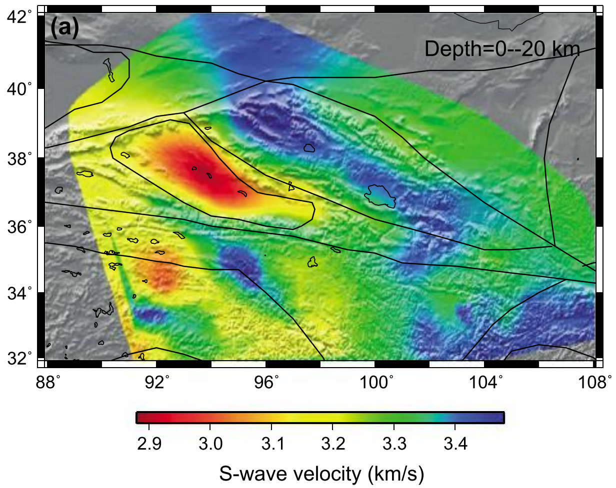

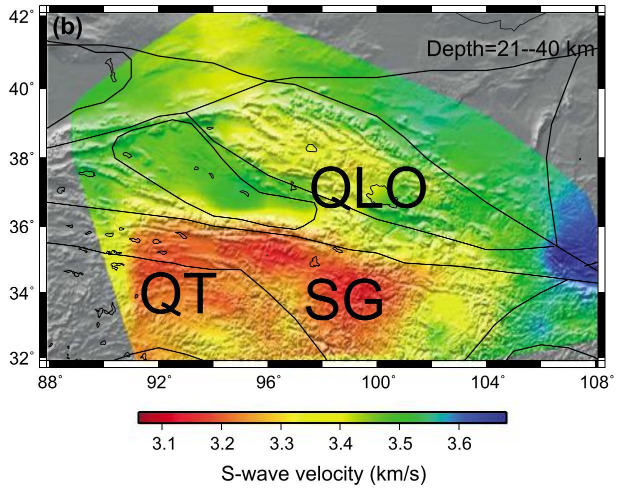

20-40 km

40-65 km

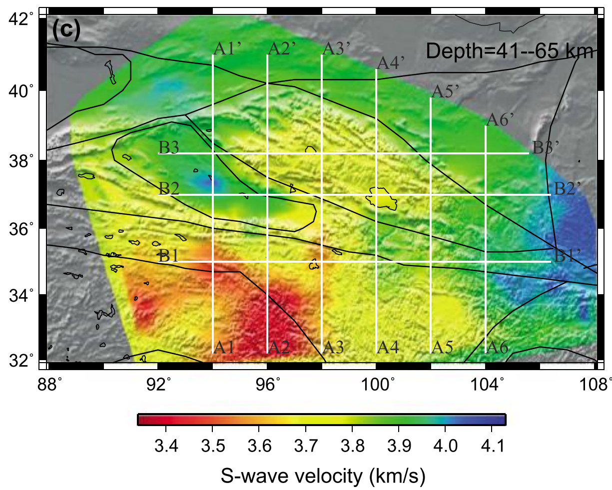

Li et al. (2014)

Joint inversion: synthetic tests

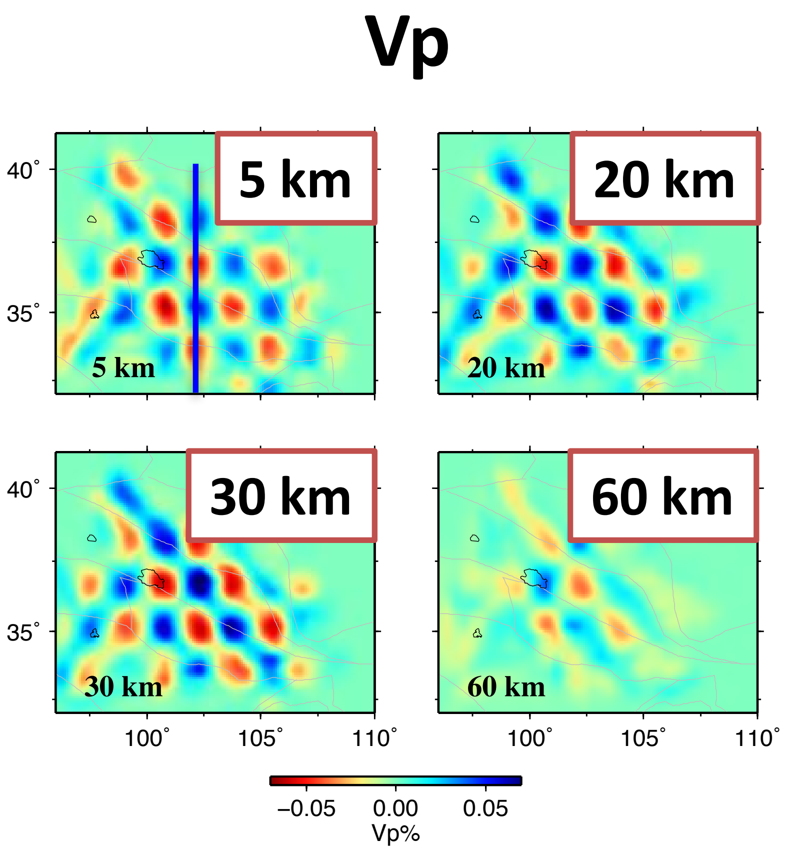

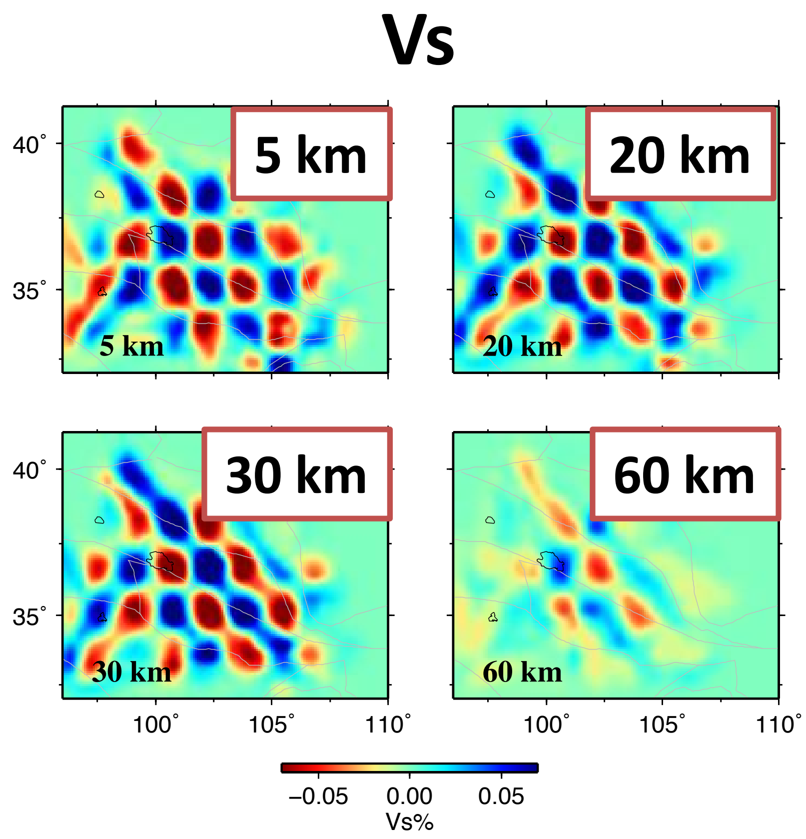

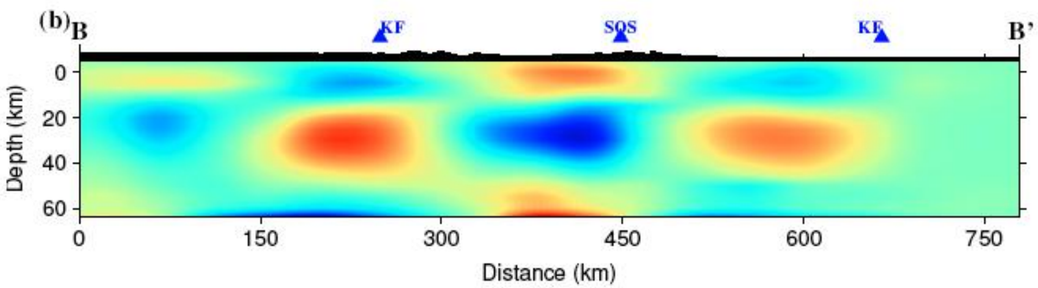

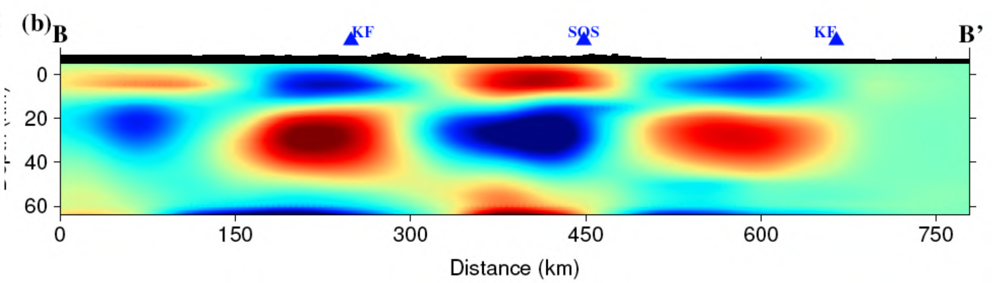

Output model for Vp/Vs

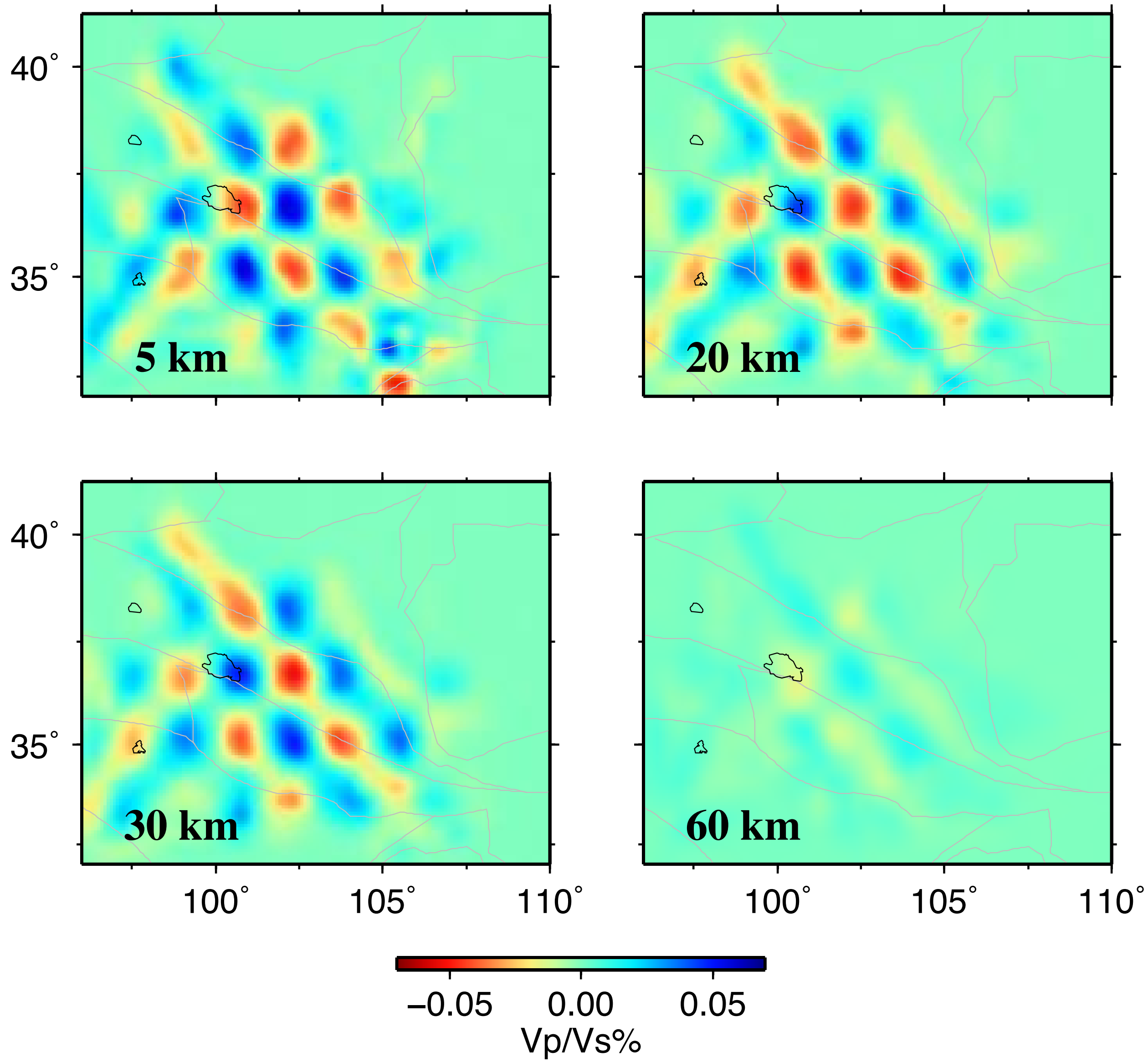

Horizontal slices at different depths

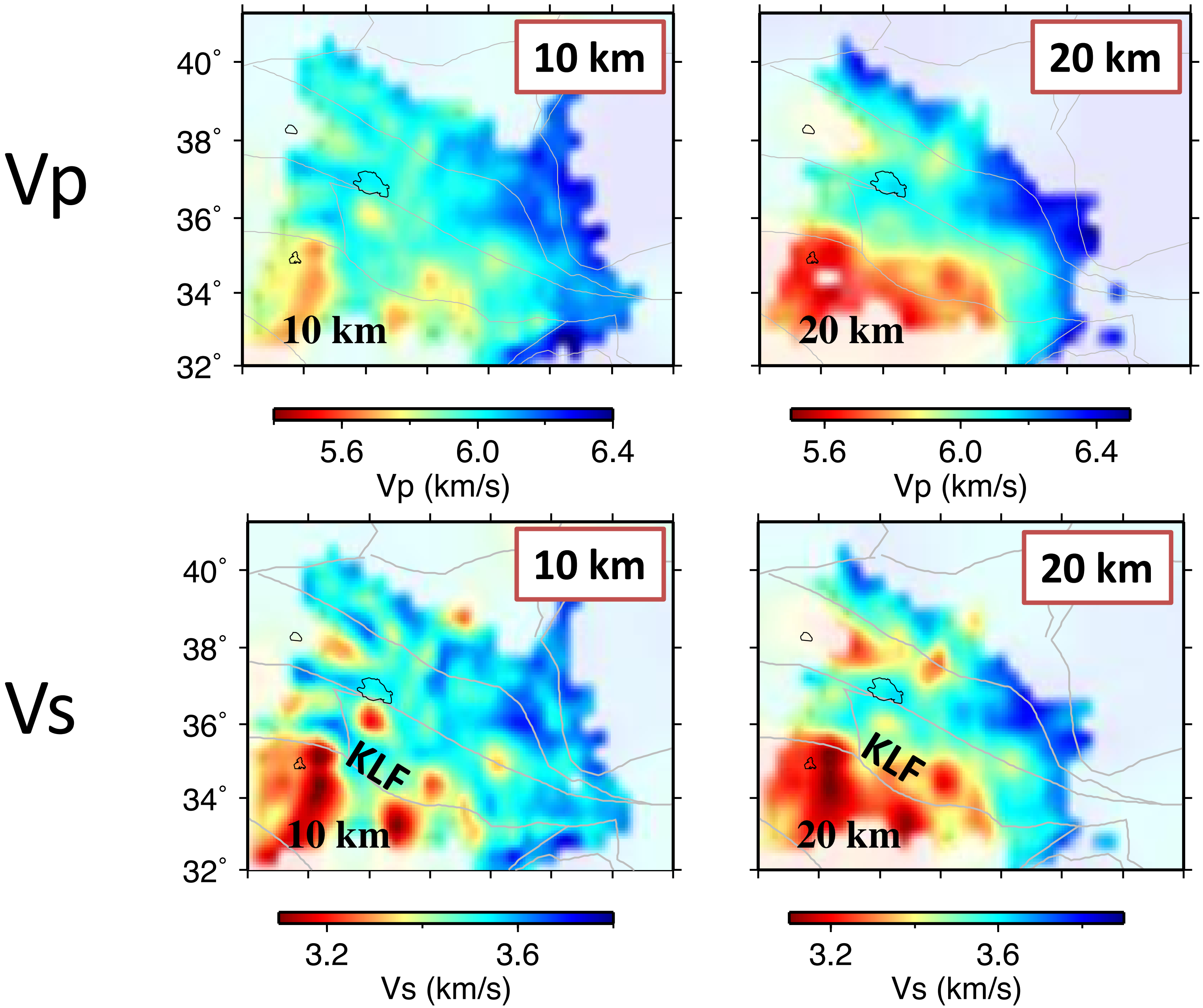

Horizontal slices at different depths

Vp

Vs

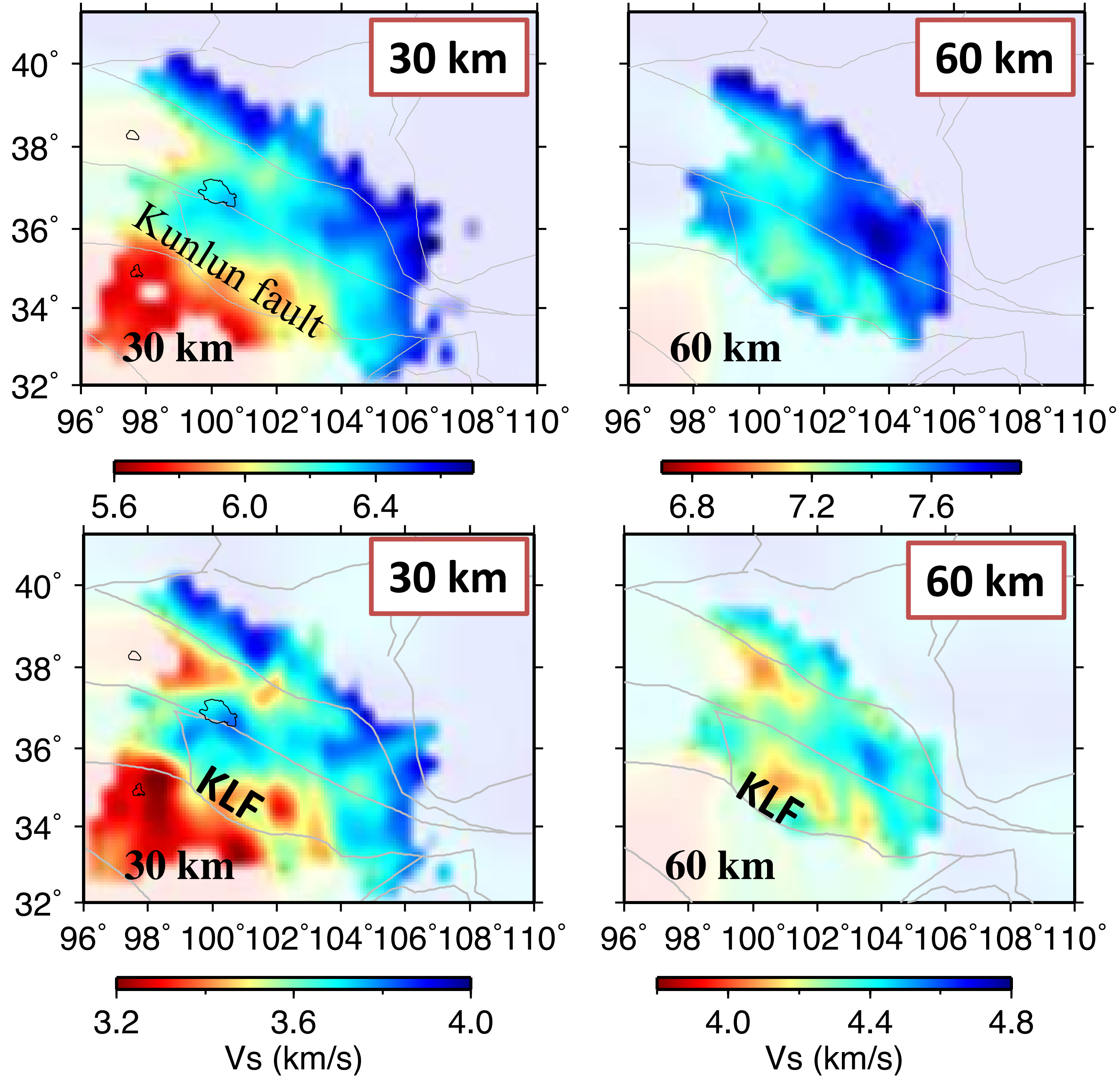

Crustal LVZ: limited distribution, mainly SW of the Kunlun fault

Vp/Vs model at different depths

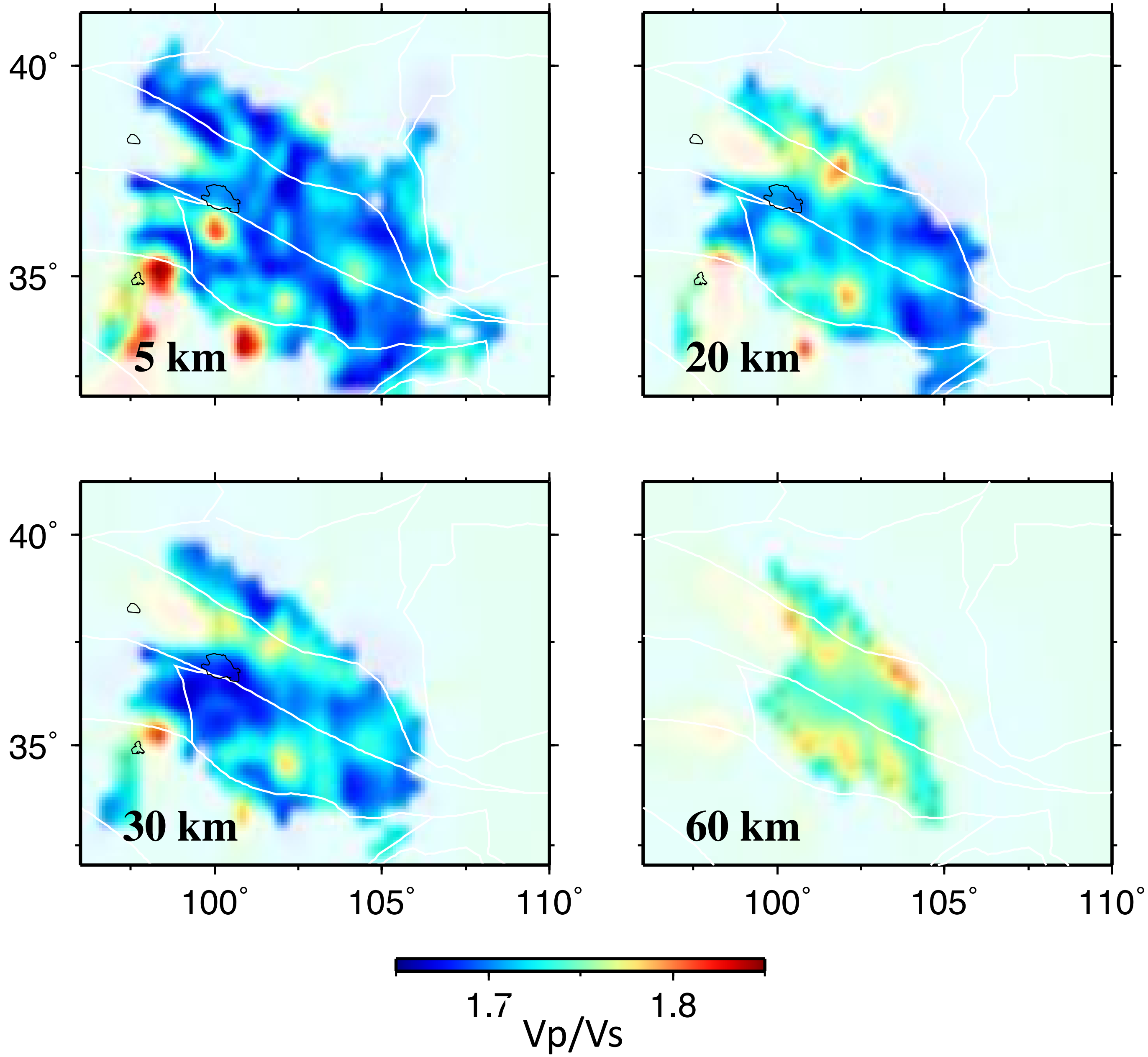

Normal or lower crustal Vp/Vs：probably more felsic component

Vertical slices: Vs

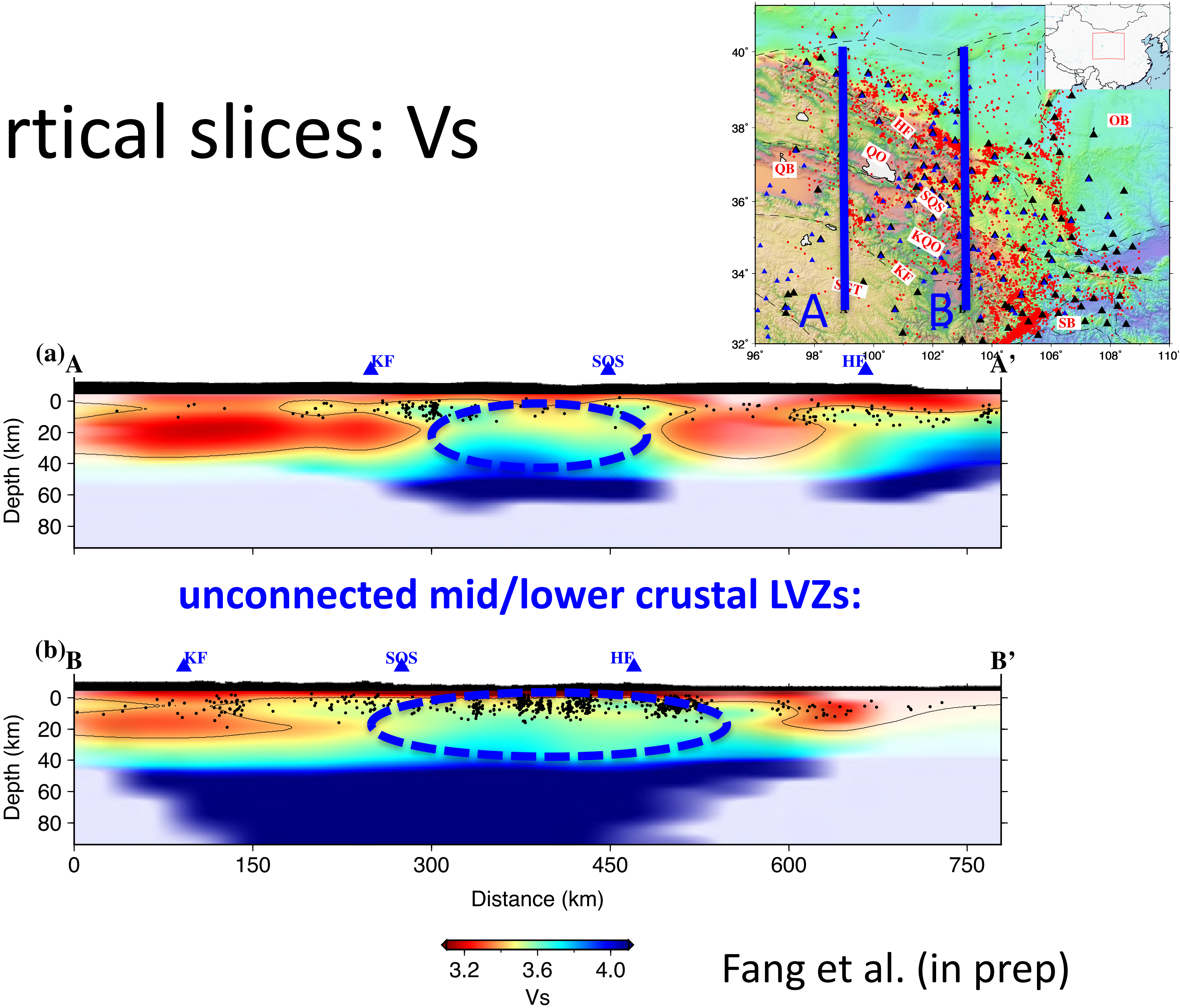

unconnected mid/lower crustal LVZs:

Fang et al. (in prep)

Vertical slices: Vp/Vs

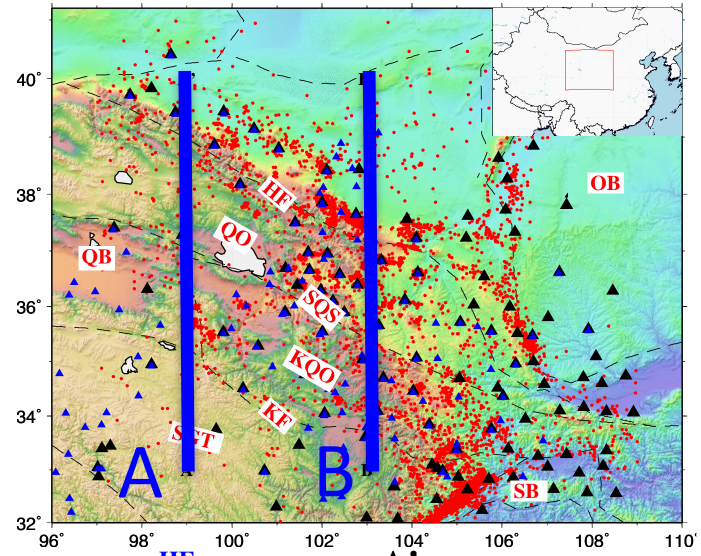

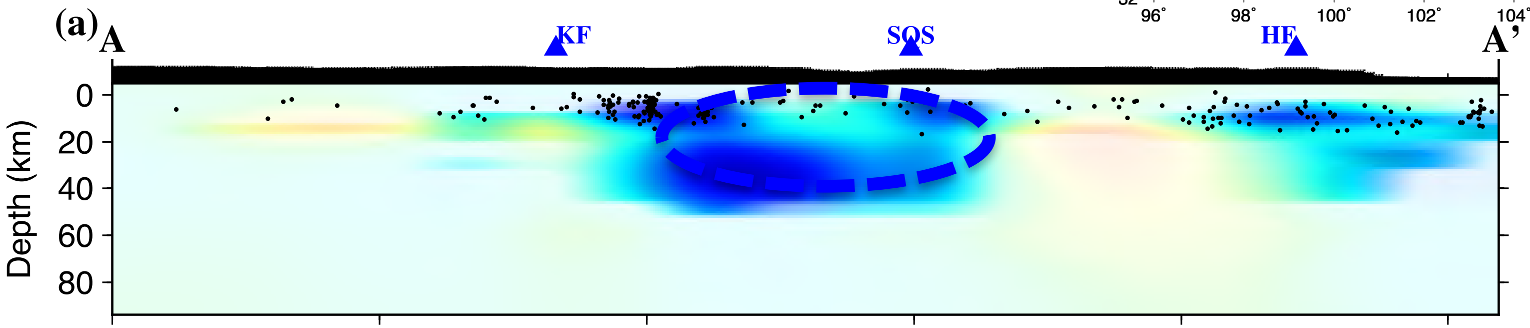

Normal to lower Vp/Vs: more felsic component

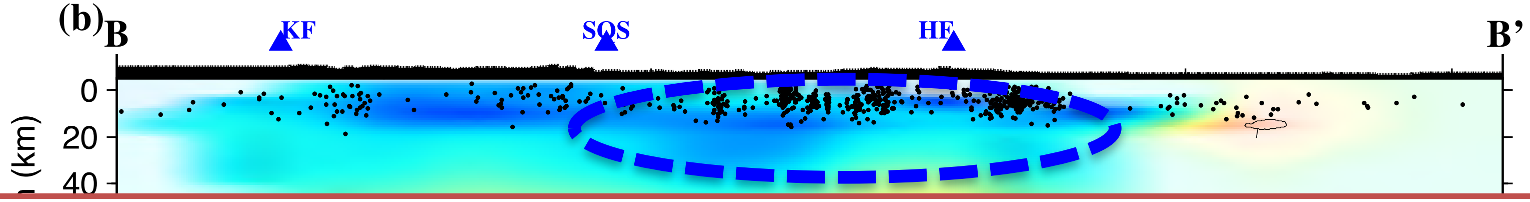

Together with normal crustal Vs, widespread northeastward crustal channel flow is unlikely!

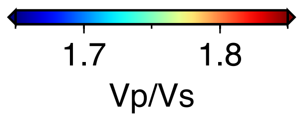

Fang et al. (in prep)

Outline

1. Joint body & surface wave traveltime tomography for 3-D Vp, Vs, and Vp/Vs models: methodology and application to NE Tibet
2. Direct inversion of 3-D azimuthal and radial anisotropy from surface wave traveltime data: methodology to SE Tibet

Azimuthal Anisotropy

HTI medium: horizontal sym. axis

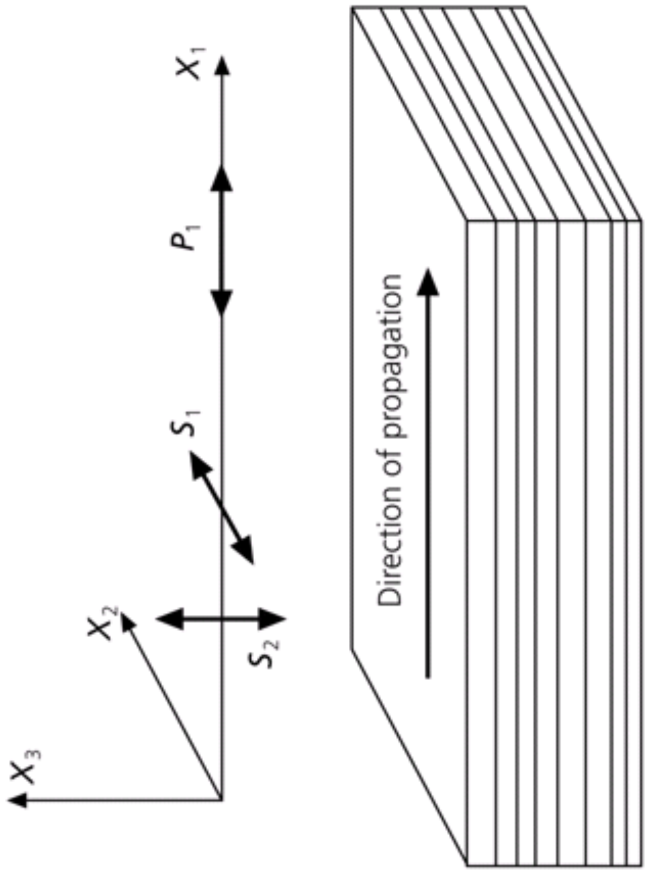

Radial Anisotropy

VTI medium: vertical sym. axis

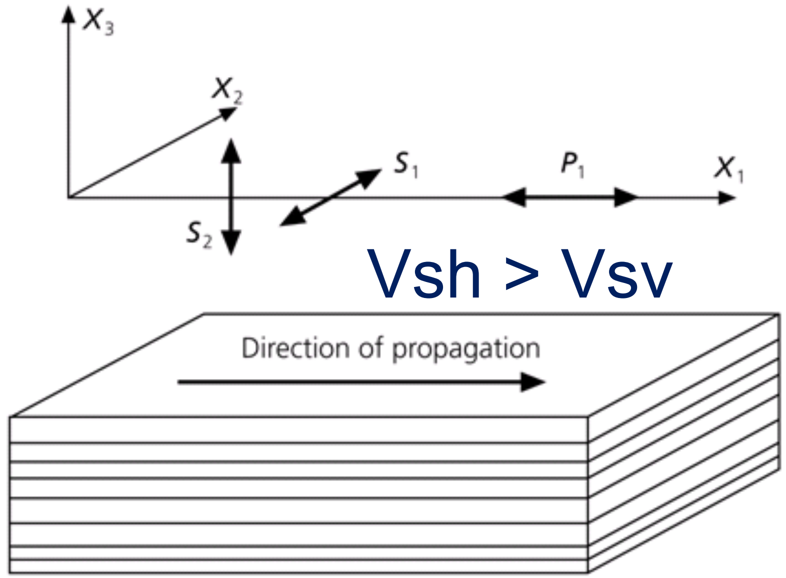

Vsh > Vsv

Causes for seismic anisotropy: cracks, layering, shape or lattice preferred orientation

Methods for seismic anisotropy: local S-wave or XKS splitting, receiver functions (Pms), body wave traveltimes, surface wave dispersion, etc

Classical representation of Rayleigh-wave and shear-wave velocity azimuthal anisotropy

Rayleigh-wave phase velocity:

$$\delta c_{\mathrm{R}}(\omega, M, \psi) \approx a_0(\omega, M) + a_{\mathrm{c}}(\omega, M)\cos 2\psi + a_{\mathrm{s}}(\omega, M)\sin 2\psi,$$

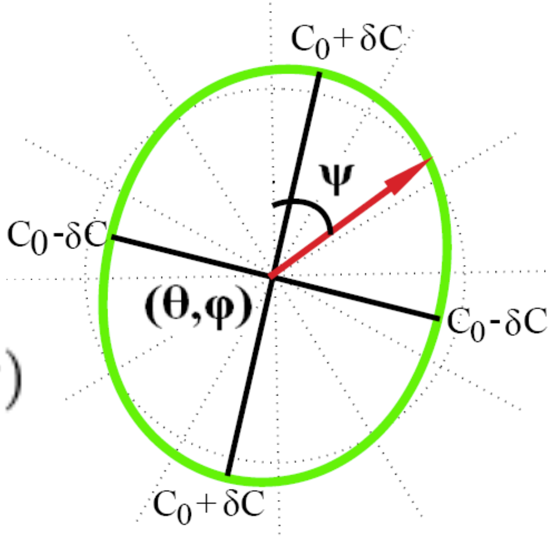

$$\delta c_{\mathrm{R}}(M, \omega, \psi) \approx \int_0^H \left[\frac{\partial c_{\mathrm{R}}(\omega)}{\partial A}(\delta A + B_{\mathrm{c}}\cos 2\psi + B_{\mathrm{s}}\sin 2\psi) + \frac{\partial c_{\mathrm{R}}(\omega)}{\partial L}(\delta L + G_{\mathrm{c}}\cos 2\psi + G_{\mathrm{s}}\sin 2\psi) + \frac{\partial c_{\mathrm{R}}}{\partial C}\delta C\right]\mathrm{d}z$$

$$\boxed{A = \rho V_{PH}^2, C = \rho V_{PV}^2, L = \rho V_{SV}^2}$$

Shear-wave velocity:

$$\hat{\beta}_{\mathrm{SV}} \approx V_{\mathrm{SV}}\left(1 + \frac{G_{\mathrm{c}}}{2L}\cos 2\psi + \frac{G_{\mathrm{s}}}{2L}\sin 2\psi\right) = V_{\mathrm{SV}}[1 + \Lambda_{\mathrm{SV}}\cos 2(\psi - \phi_{\mathrm{F}})]$$

Smith & Dahlen (1973)
Montagner & Nataf (1986)

1-D depth sensitivity kernels

Normal mode／surface wave mode theory

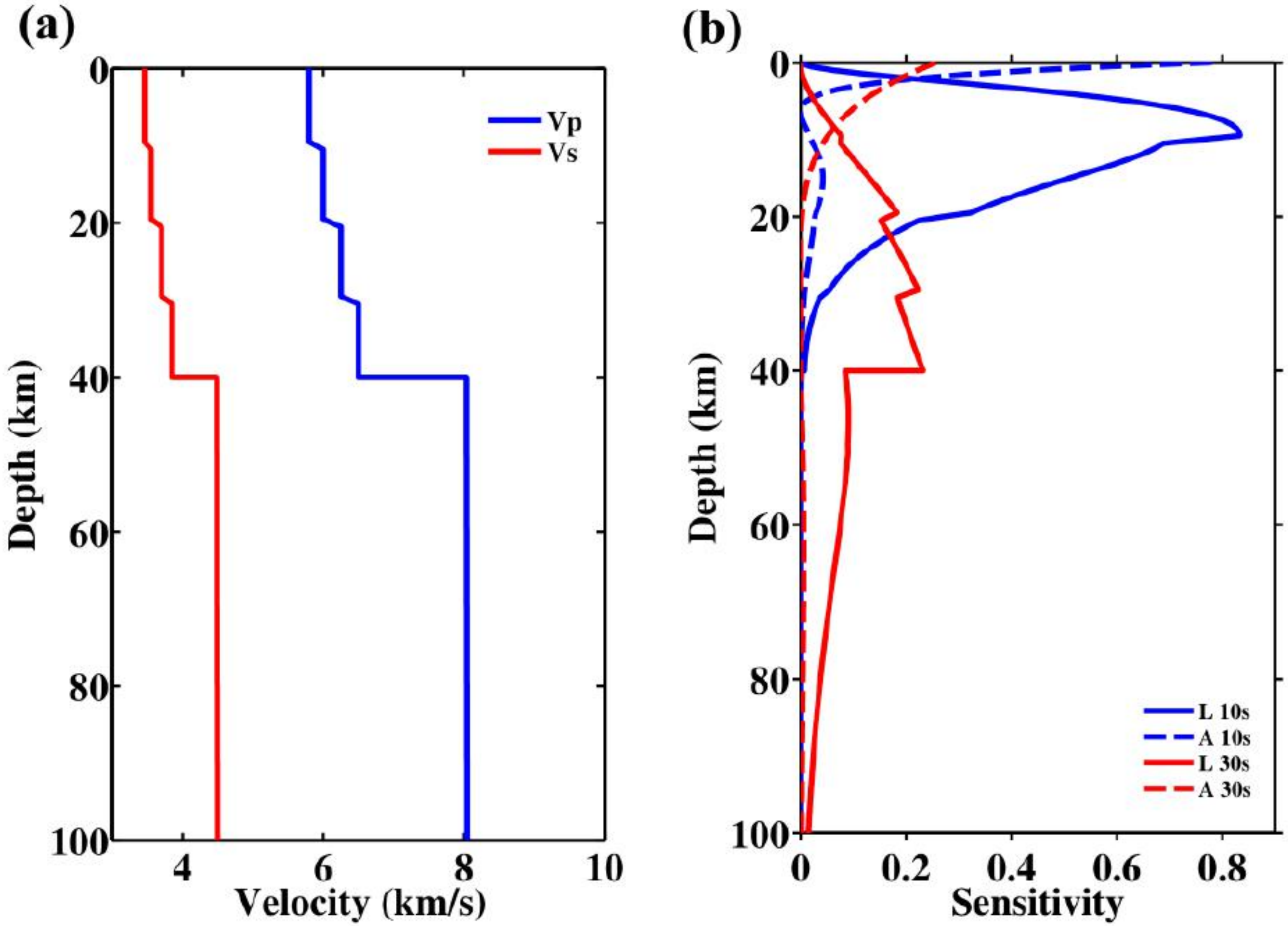

$$\frac{\partial c_k(\omega)}{\partial A_k(z)}$$

$$\frac{\partial c_k(\omega)}{\partial L_k(z)}$$

Weak azimuthal anisotropy： $\hat{V}_{SV} \approx V_{SV}\left(1 + \frac{G_c}{2L}cos2\psi + \frac{G_s}{2L}sin2\psi\right)$

Traditional two-step inversion for Vs azimuthal anisotropy from Rayleigh waves

Mix-path phase velocity dispersion curves

Step 1

2-D phase v maps with azim. anis.

Pointwise inversion for 1-D Vs model and azim. aniso., then combined for 3-D model

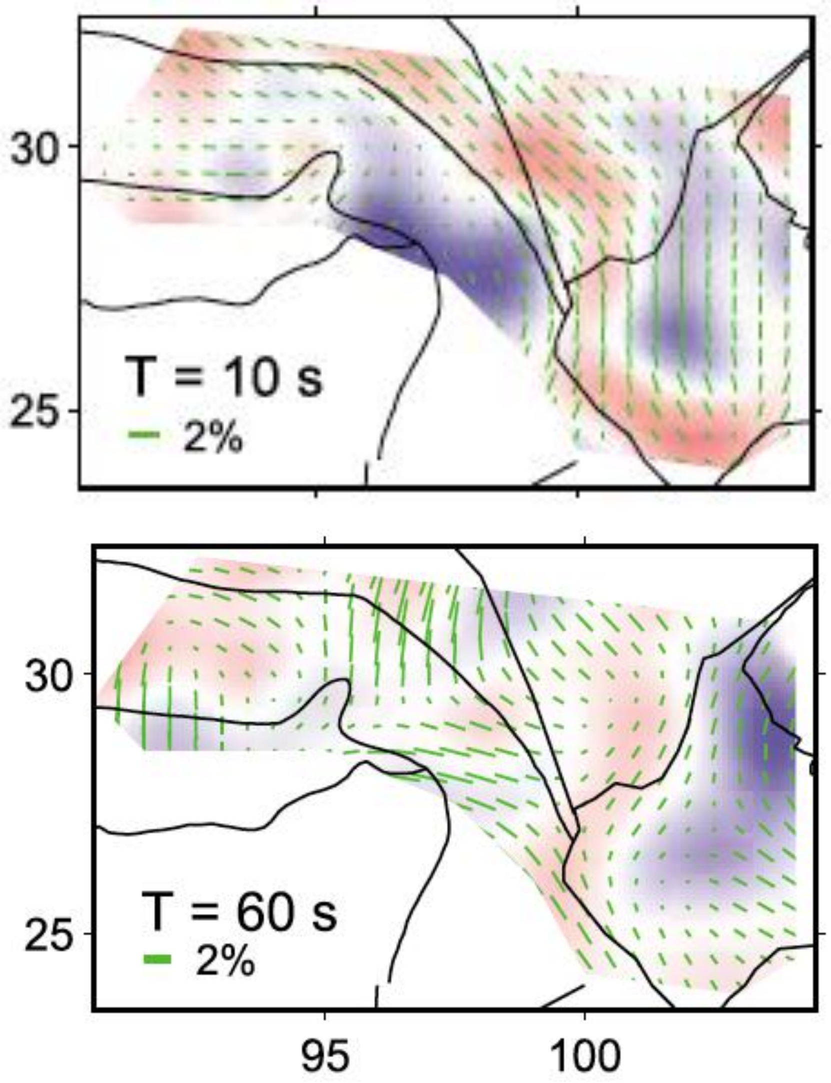

Yao et al. (2010 , JGR)

Traditional two-step inversion for Vs azimuthal anisotropy from Rayleigh waves

Mix-path phase velocity dispersion curves

↓

2-D phase v maps with azim. anis.

↓ **Step 2**

Pointwise inversion for 1-D Vs model and azim. aniso., then combined for 3-D model

Yao et al. (2010 , JGR) : linearized

Yao (2015 , EQS) : NA

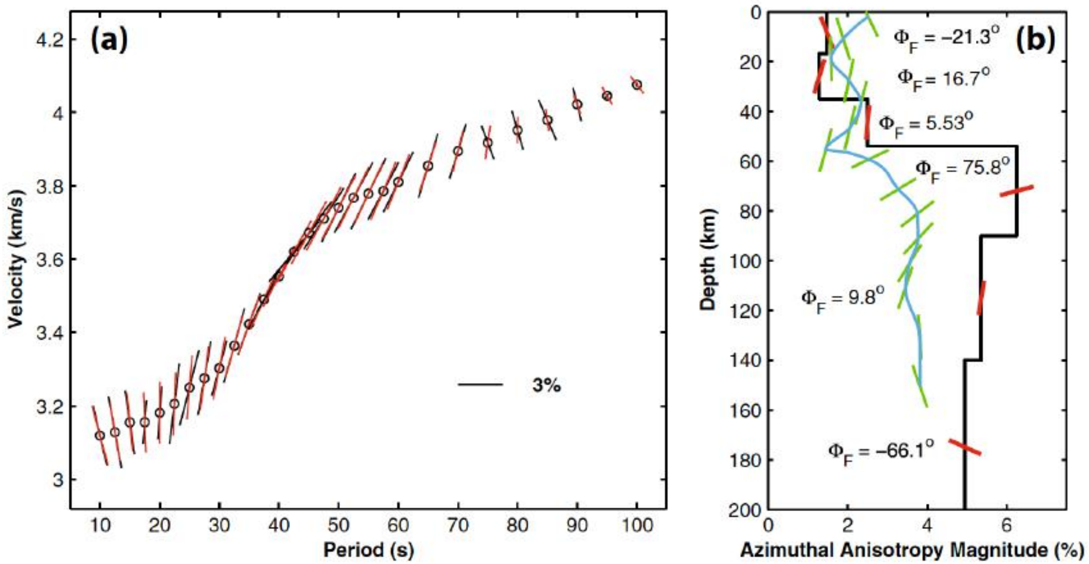

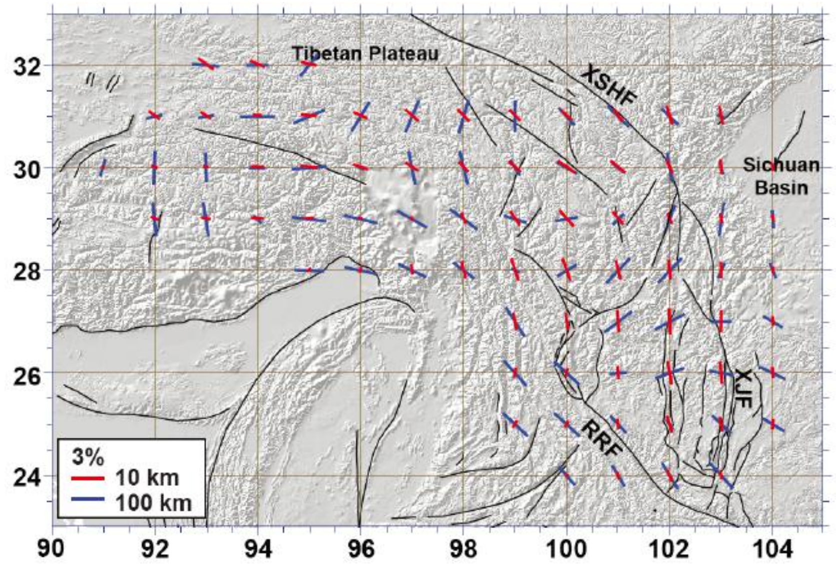

Direct inversion for 3-D Vs azimuthal anisotropy based on raytracing from dispersion data

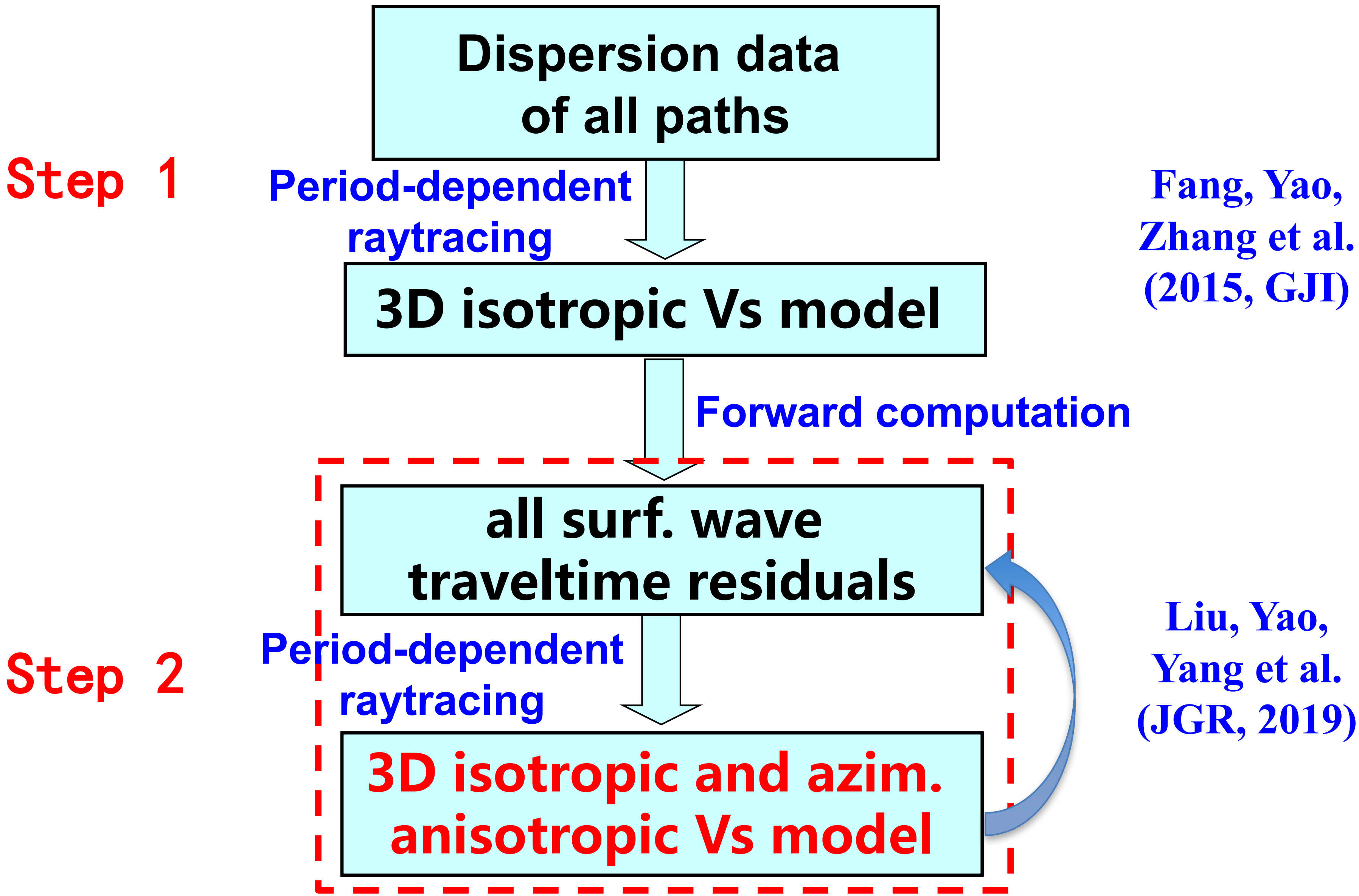

Step 1. All dispersion data → 3-D isotropic Vs

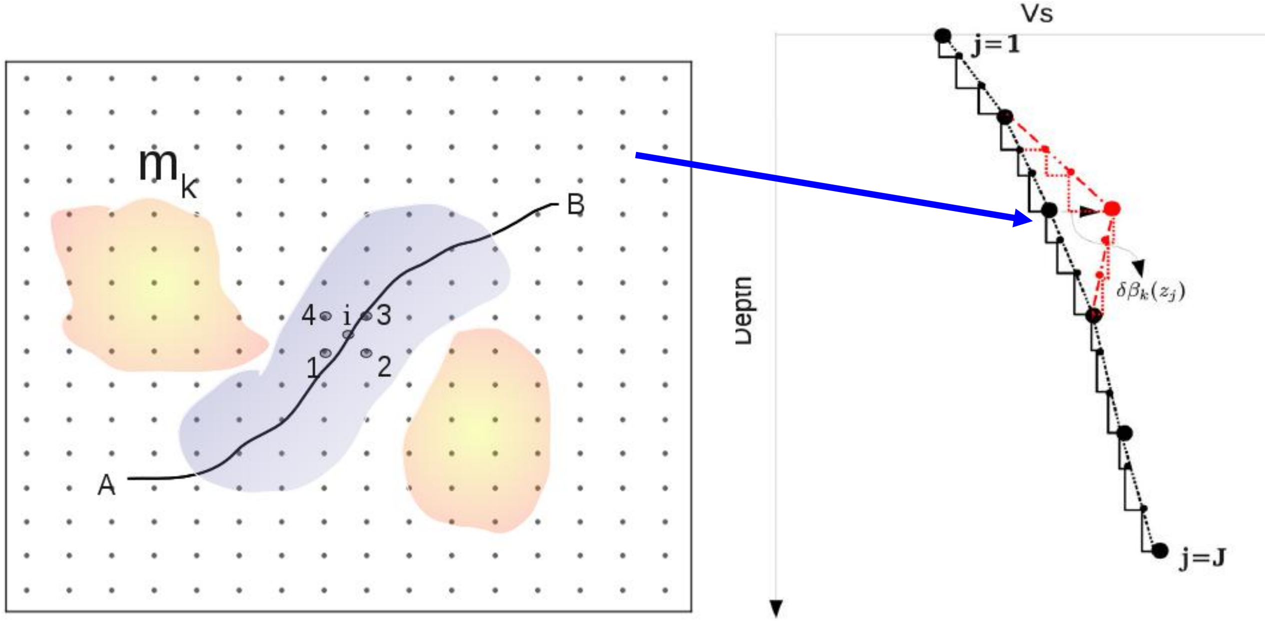

$$\delta t_i(w) = \sum_{k=1}^{K}\left(-\frac{\nu_{ik}}{C_k^2(\omega)}\right)\sum_{j=1}^{J}\left[R_\alpha(z_j)\frac{\partial C_k(\omega)}{\partial \alpha_k(z_j)} + R_\rho(z_j)\frac{\partial C_k(\omega)}{\partial \rho_k(z_j)} + \frac{\partial C_k(\omega)}{\partial \beta_k(z_j)}\right]\Bigg|_{\Theta_k} \delta\beta_k(z_j) = \sum_{l=1}^{M} G_{il} m_l, \quad (10)$$

Fang, Yao, et al. (2015, GJI)

Step 2. All traveltime residual data → 3-D isotropic and azimuthally anisotropic Vs

Based on the 3-D ref. model from Step 1

$$\delta t_i(\omega) = t_i^{obs}(\omega) - t_i^{ref}(\omega) \approx \sum_{k=1}^{K} \frac{-\mu_{ik}}{(c_0^k(\omega))^2} \left(\delta c_k(\omega) + a_1^k(\omega) cos2\psi + a_2^k(\omega) sin2\psi\right)$$

$$= \sum_{k=1}^{K} \frac{-\mu_{ik}}{(c_0^k(\omega))^2} \left(\boxed{\delta c_k^{ETI}(\omega)} + \boxed{\delta c_k^{AA}(\omega,\psi)}\right).$$

$$\delta c_k^{ETI}(\omega) = \int_0^\infty \left(\frac{\partial c_k(\omega)}{\partial \alpha_k(z)} \delta\alpha_k(z) + \frac{\partial c_k(\omega)}{\partial \beta_k(z)} \delta\beta_k(z) + \frac{\partial c_k(\omega)}{\partial \rho_k(z)} \delta\rho_k(z)\right) dz,$$

$$\delta c_k^{AA}(\omega) = \int_0^\infty \left\{\left(B_c^k \frac{\partial c_k(\omega)}{\partial A_k} + G_c^k \frac{\partial c_k(\omega)}{\partial L_k}\right) cos2\psi + \left(B_s^k \frac{\partial c_k(\omega)}{\partial A_k} + G_s^k \frac{\partial c_k(\omega)}{\partial L_k}\right) sin2\psi + (H_c^k cos2\psi + H_s^k sin2\psi) \frac{\partial c_k(\omega)}{\partial F_k}\right\} dz,$$

Step 2. All traveltime residual data → 3-D isotropic and azimuthally anisotropic Vs

some simplifications and finally …

$$\delta t_i(\omega) = \sum_{k=1}^{K} \frac{-\mu_{ik}}{(c_0^k(\omega))^2} \sum_{j=1}^{J} \Bigg\{ \Bigg[\left(\int_{z_j}^{z_{j+1}} \frac{\partial c_k(\omega)}{\partial \alpha_k(z)} dz \right) R_\alpha(z_j) + \left(\int_{z_j}^{z_{j+1}} \frac{\partial c_k(\omega)}{\partial \beta_k(z)} dz \right) + \left(\int_{z_j}^{z_{j+1}} \frac{\partial c_k(\omega)}{\partial \rho_k(z)} dz \right) R_\rho(z_j) \Bigg] \underline{\delta\beta_k(z_j)} + \eta_{ik} \left[\left(\int_{z_j}^{z_{j+1}} \frac{\partial c_k(\omega)}{\partial A_k(z)} dz \right) A_k(z_j) + \left(\int_{z_j}^{z_{j+1}} \frac{\partial c_k(\omega)}{\partial L_k(z)} dz \right) L_k(z_j) \right] \underline{\frac{G_C^k(z_j)}{L_k(z_j)}} + \xi_{ik} \left[\left(\int_{z_j}^{z_{j+1}} \frac{\partial c_k(\omega)}{\partial A_k(z)} dz \right) A_k(z_j) + \left(\int_{z_j}^{z_{j+1}} \frac{\partial c_k(\omega)}{\partial L_k(z)} dz \right) L_k(z_j) \right] \underline{\frac{G_S^k(z_j)}{L_k(z_j)}} \Bigg\},$$

$$\boxed{\rightarrow \mathbf{d} = \mathbf{G}\,\mathbf{m}}$$

$$\mathbf{m} = \left[\underline{\Delta\beta_1(z_j) \ldots \Delta\beta_1(z_J) \ldots \Delta\beta_K(z_J)} \;\; \underline{\frac{G_C^1(z_1)}{L_1(z_1)} \cdots \frac{G_C^1(z_J)}{L_1(z_J)} \cdots \frac{G_C^K(z_J)}{L_K(z_J)}} \;\; \underline{\frac{G_S^1(z_1)}{L_1(z_1)} \cdots \frac{G_S^1(z_J)}{L_1(z_J)} \cdots \frac{G_S^K(z_J)}{L_K(z_J)}} \right]^T$$

Inversion matrix:

$$\begin{bmatrix} \mathbf{G}_{iso} & \mathbf{G}_{AA} \\ \lambda_1 \mathbf{L}_{iso} & \mathbf{0} \\ \mathbf{0} & \lambda_2 \mathbf{L}_{AA} \end{bmatrix} \begin{bmatrix} \boldsymbol{m}_{iso} \\ \boldsymbol{m}_{AA} \end{bmatrix} = \begin{bmatrix} \boldsymbol{d} \\ \mathbf{0} \\ \mathbf{0} \end{bmatrix}$$

Synthetic examples

Input model

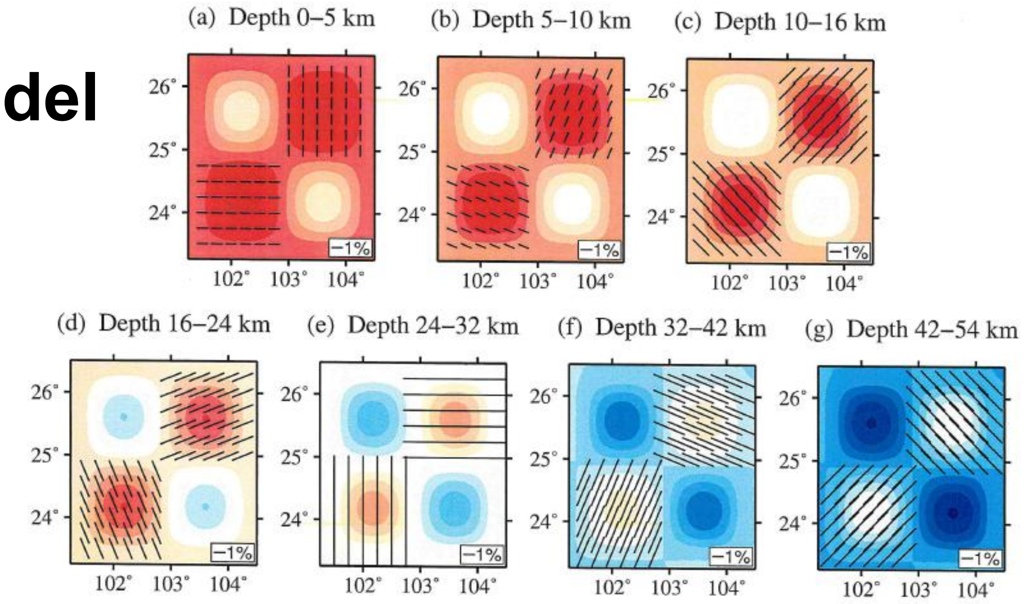

Output model: no data noise

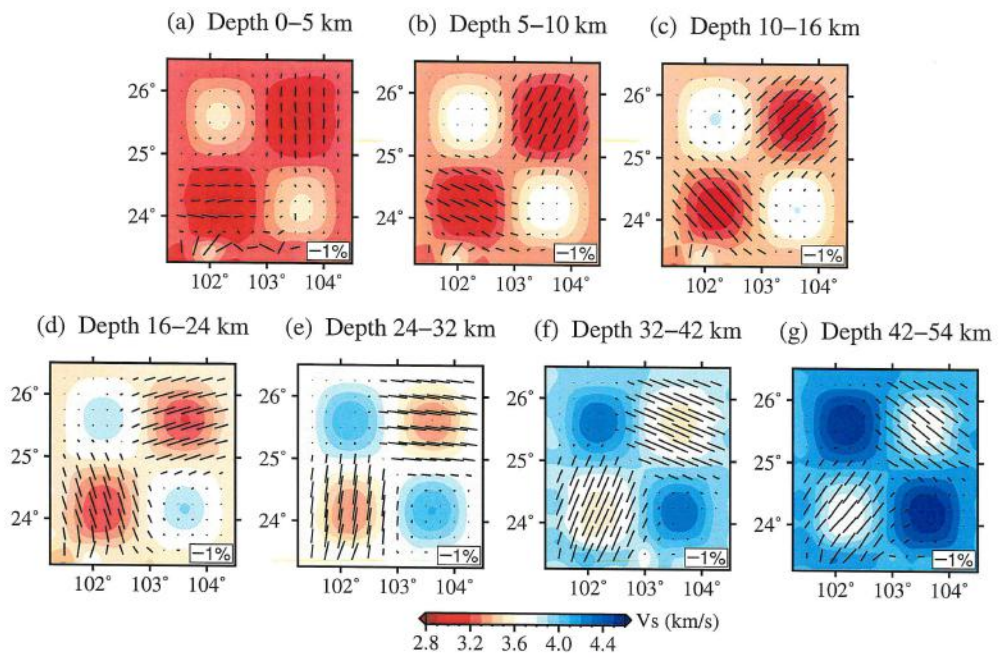

Output model: 1% data noise

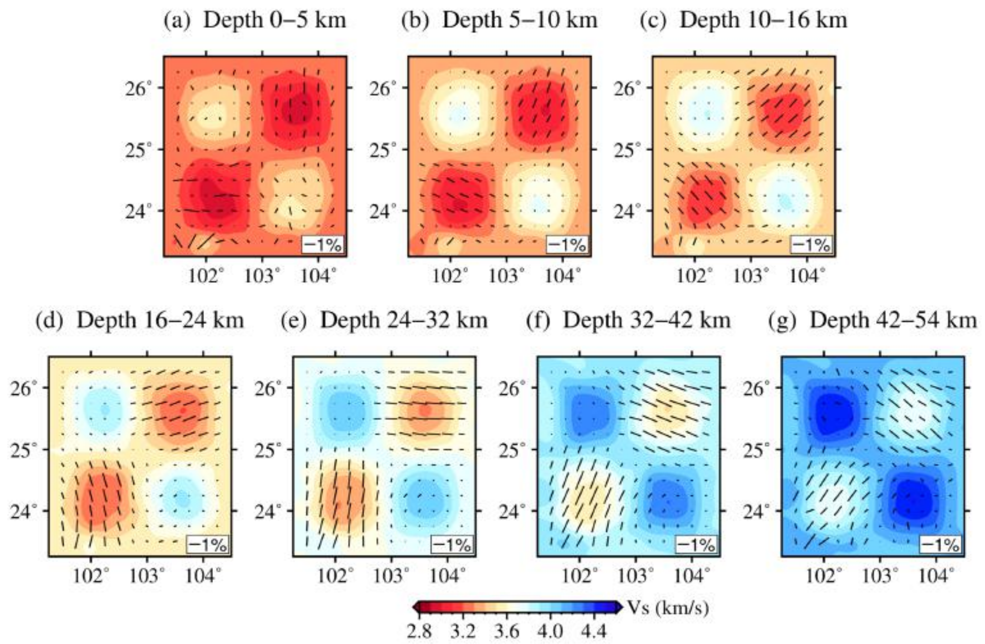

DAzimSurfTomo: Application to SE Tibet

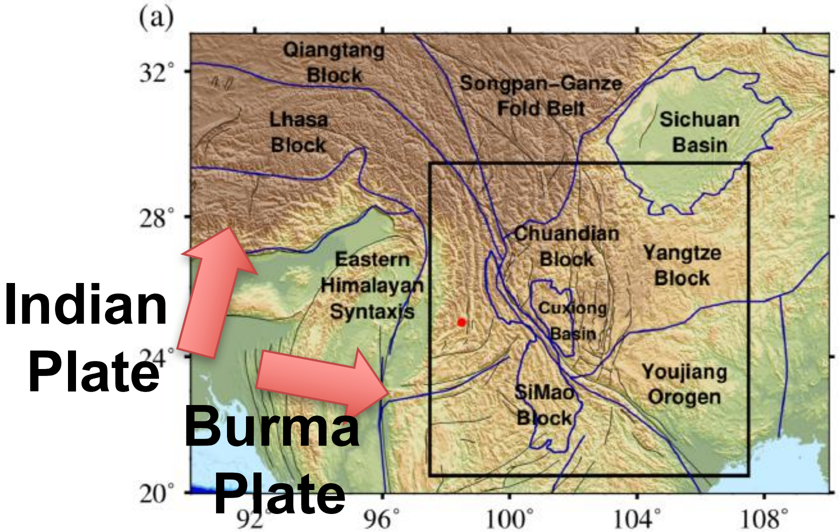

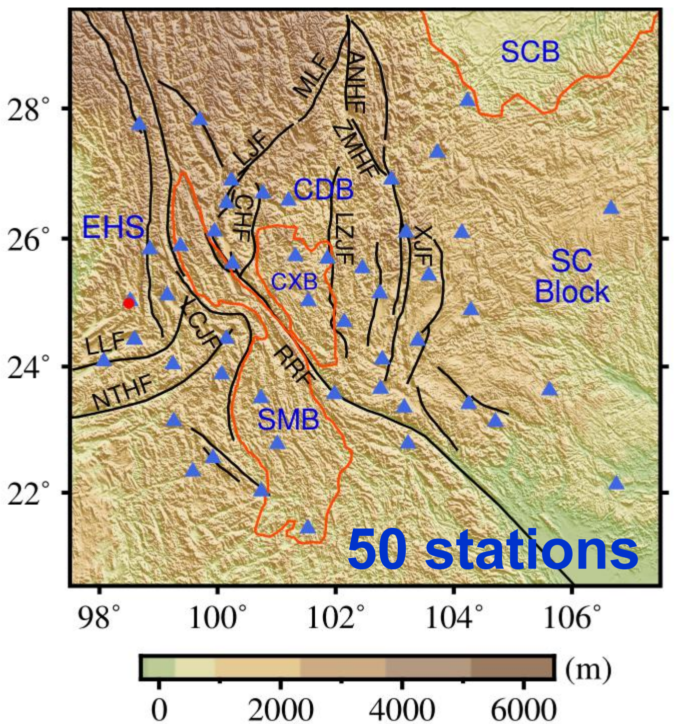

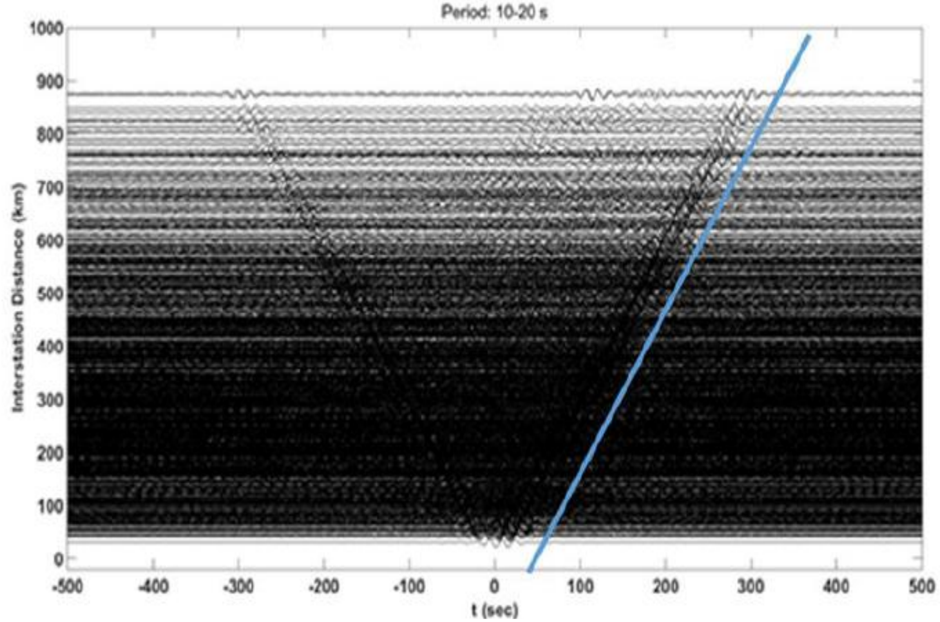

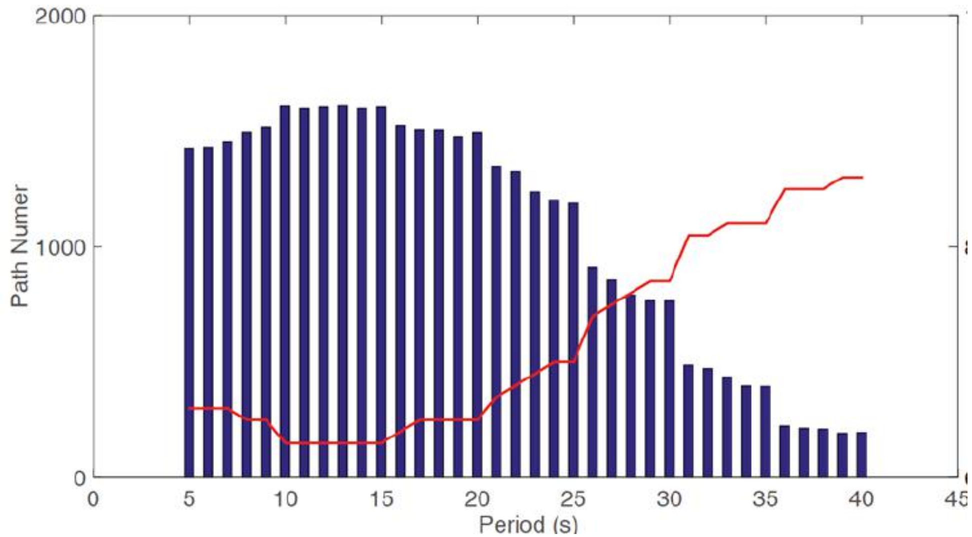

Vs model in the crust and uppermost mantle

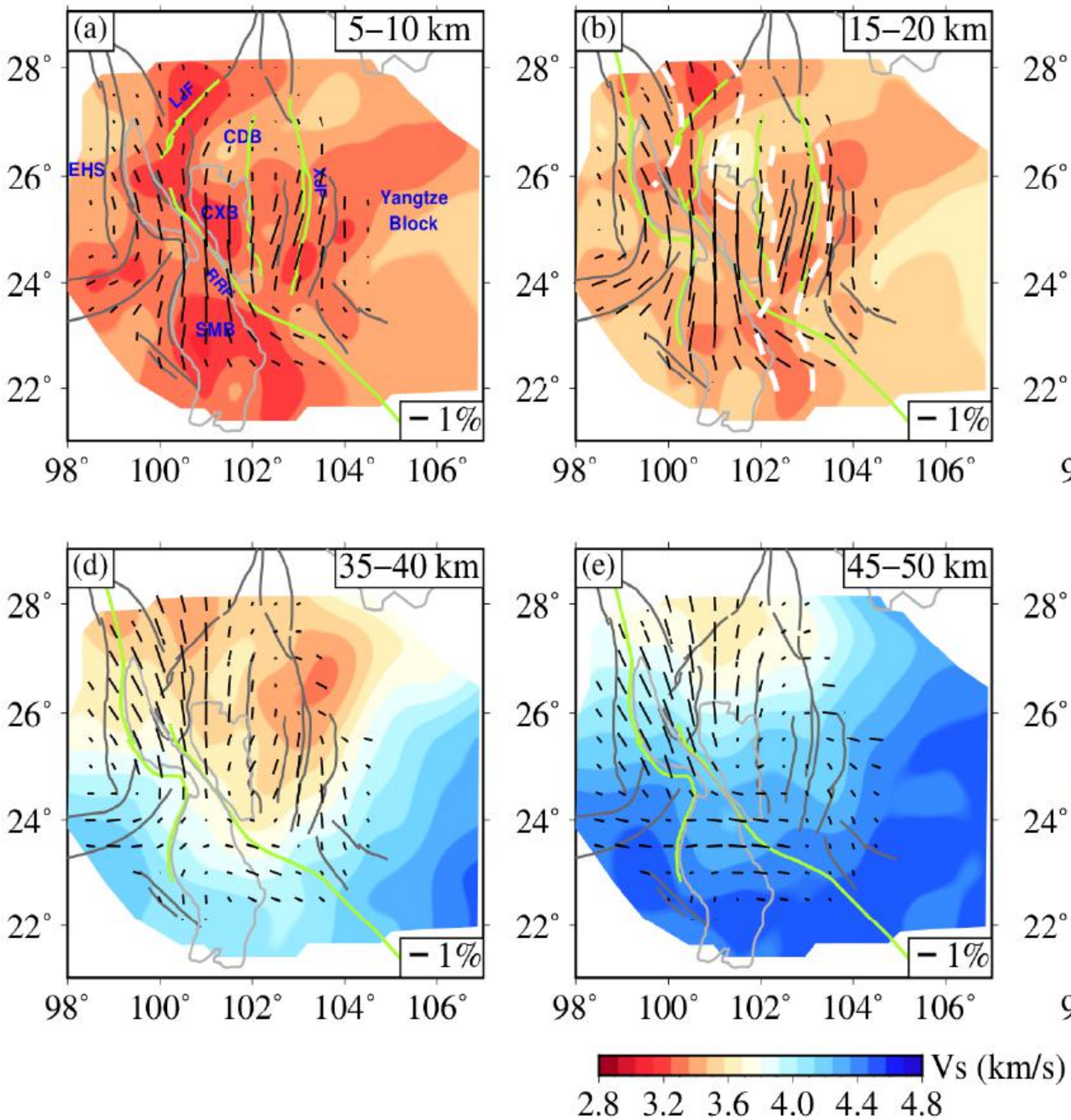

Liu, Yao,Yang et al. (JGR, 2019)

Comparison of 2-D phase v maps

computed from our 3-D model

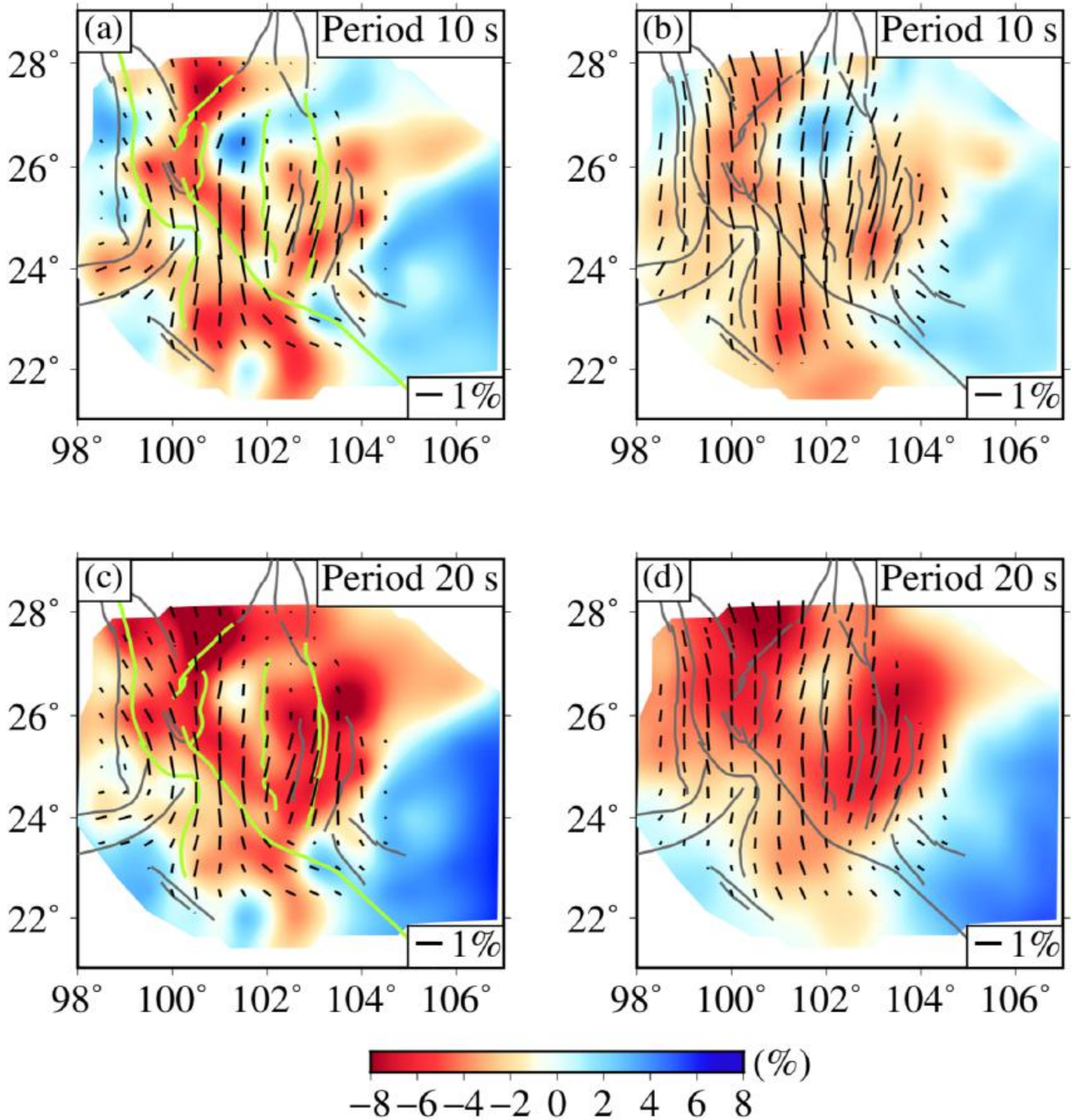

classic 2-D tomography results of Shen et al (2016)

1° x 1° checkerboard model

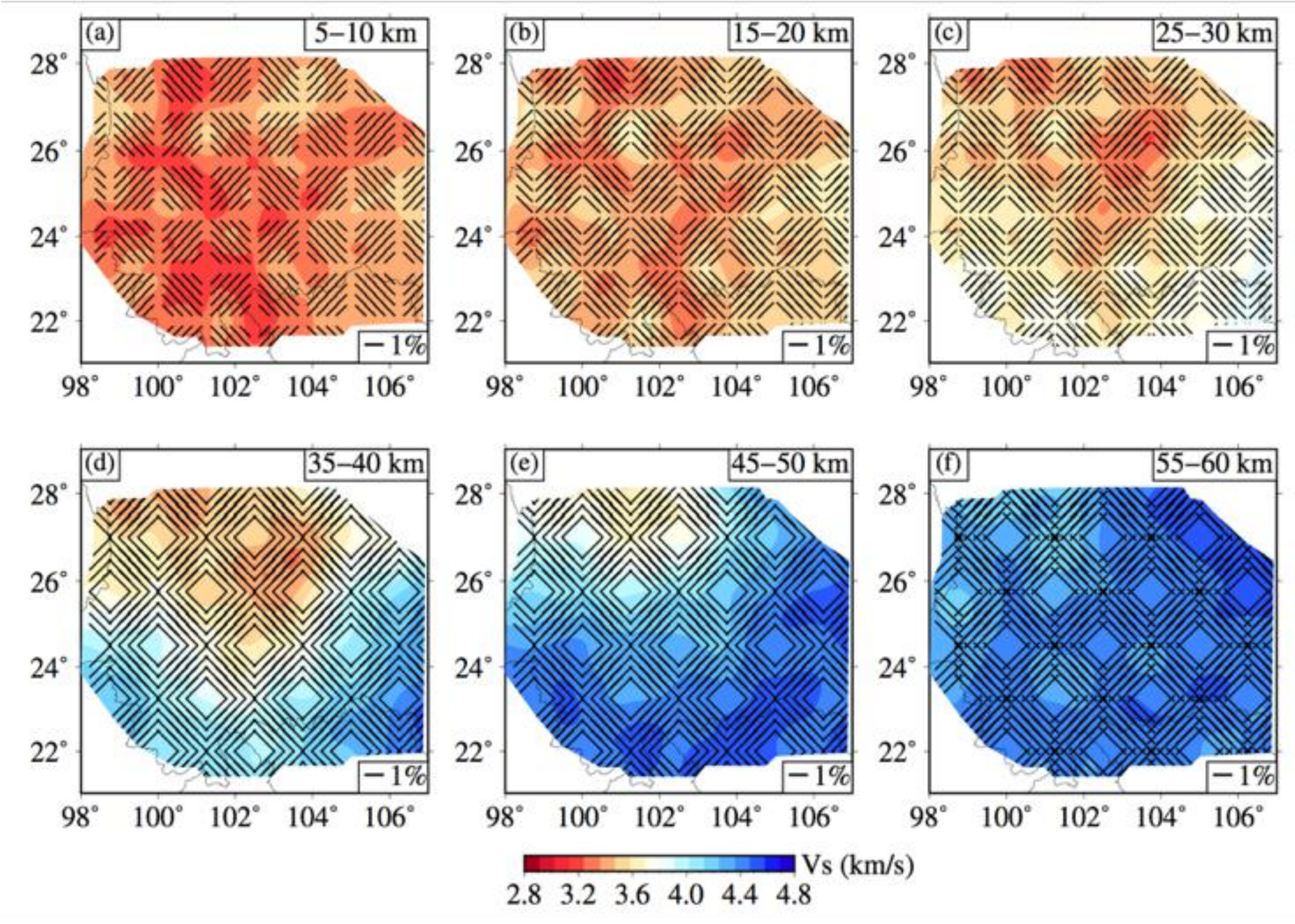

1° x 1° checkerboard recovery

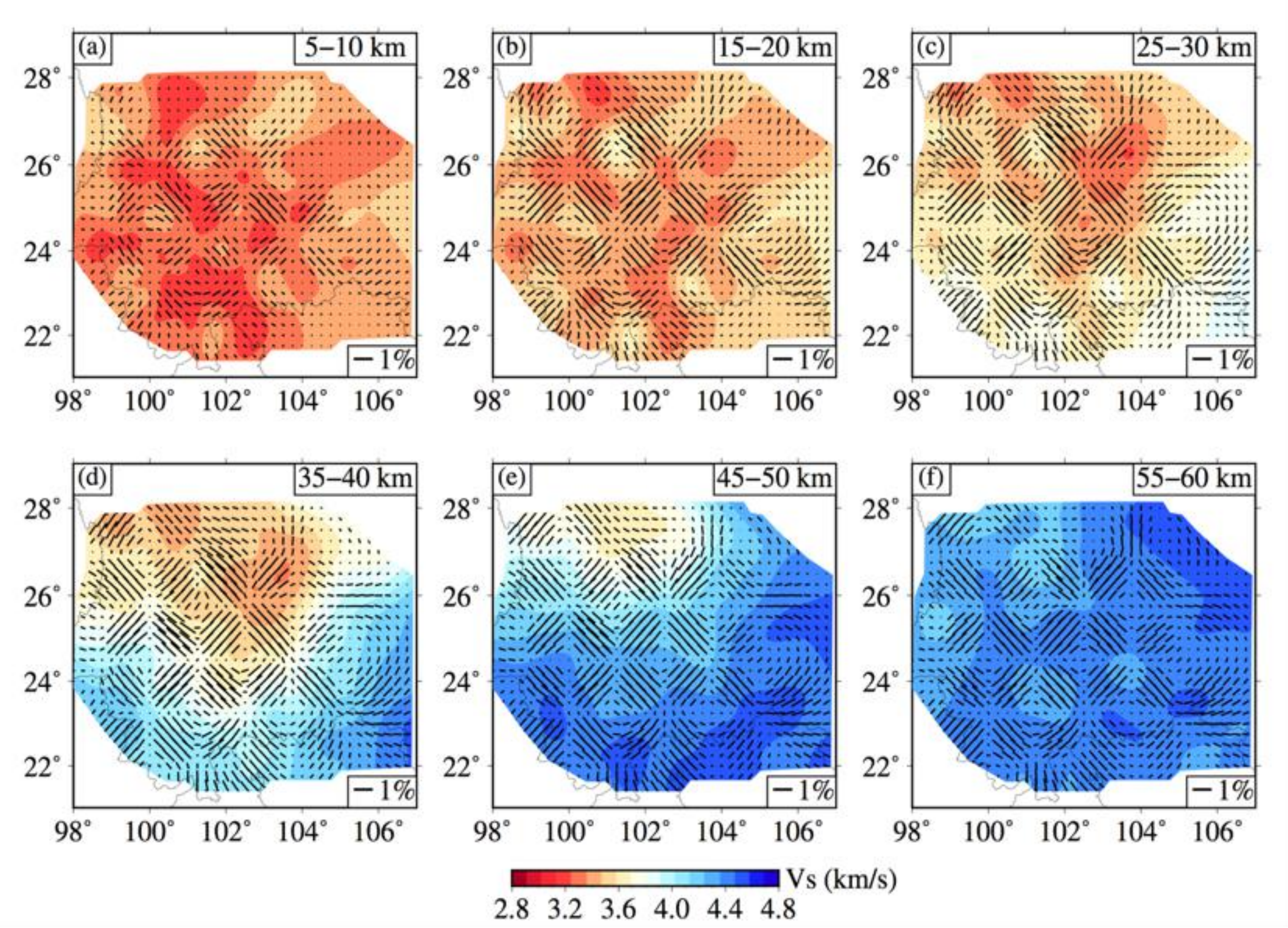

Vs Azim Aniso.
（red bars）

XKS splitting （blue bars）(Chang et al, 2016)

Apparent differences in crust and uppermost mantle azim. aniso.

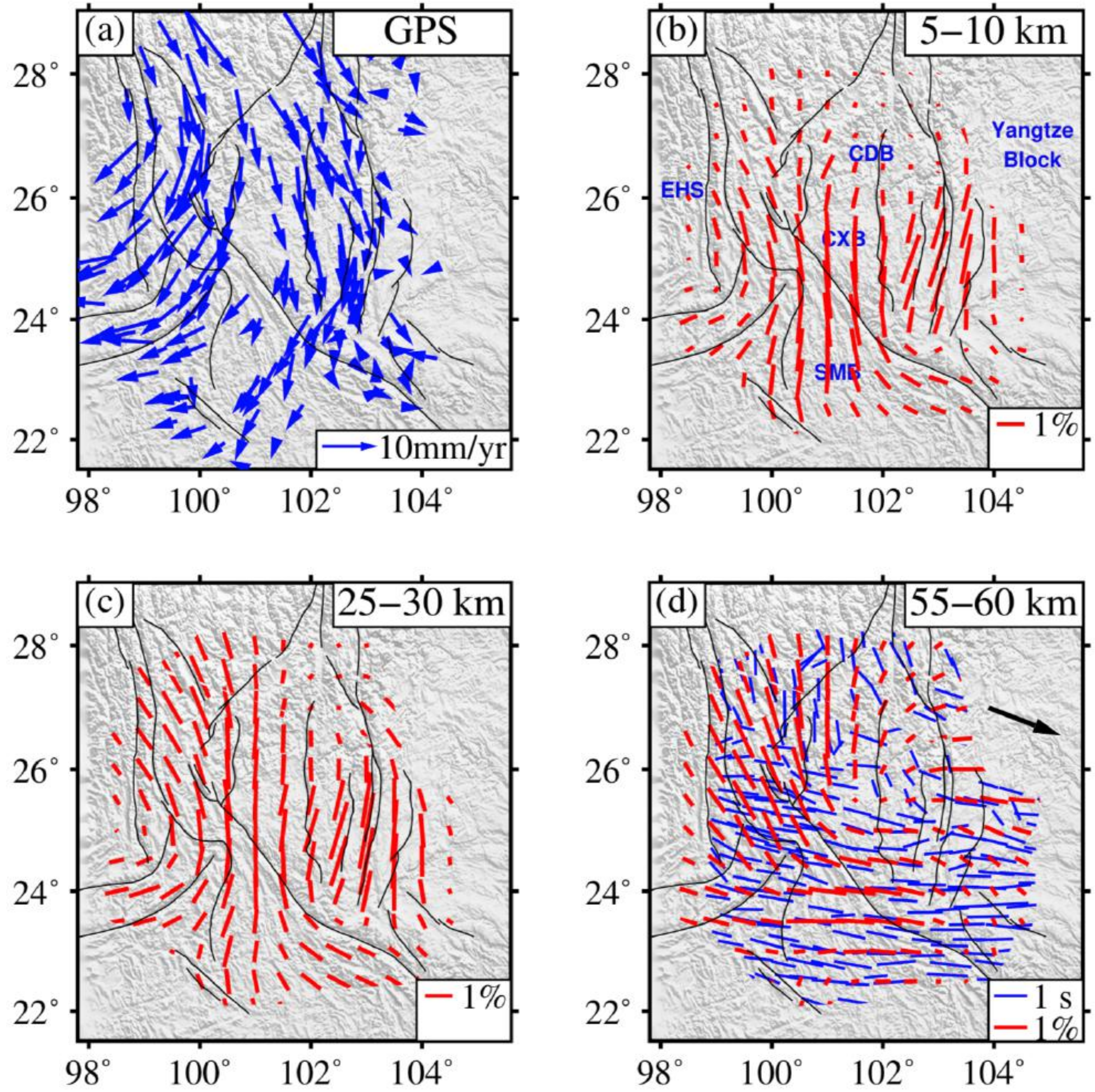

Liu, Yao, Yang et al. (JGR, 2019)

Direct inversion for 3-D Vsh and Vsv

Rayleigh
Love

$$\begin{pmatrix} \Delta\mathbf{T}_R \\ \Delta\mathbf{T}_L \end{pmatrix} = \begin{pmatrix} \mathbf{G}_{sv} & \mathbf{0} \\ \mathbf{0} & \mathbf{G}_{sh} \end{pmatrix} \begin{pmatrix} \Delta\mathbf{V}_{sv} \\ \Delta\mathbf{V}_{sh} \end{pmatrix}$$

3-D inversion: spatial smoothing added on $\Delta\mathbf{V}_{sh}$ & $\Delta\mathbf{V}_{sv}$

$$\gamma = \frac{V_{sh}}{V_{sv}}$$ **and** $$\left(\frac{V_{sh}+V_{sv}}{2}, \frac{2(V_{sh}-V_{sv})}{V_{sh}+V_{sv}} \right)$$

Radial anisotropy : direct division → large uncertainty

Direct inversion for 3-D Vs radial anisotropy

$$\gamma = \frac{V_{sh}}{V_{sv}} \Rightarrow \Delta\mathbf{V}_{sh} = \gamma \cdot \Delta\mathbf{V}_{sv} + \mathbf{V}_{sv} \cdot \Delta\gamma$$

$$\begin{pmatrix} \Delta\mathbf{T}_R \\ \Delta\mathbf{T}_L \end{pmatrix} = \begin{pmatrix} \mathbf{G}_{sv} & \mathbf{0} \\ \mathbf{0} & \mathbf{G}_{sh} \end{pmatrix} \begin{pmatrix} \Delta\mathbf{V}_{sv} \\ \Delta\mathbf{V}_{sh} \end{pmatrix}$$

$$\Downarrow$$

$$\begin{pmatrix} \Delta\mathbf{T}_R \\ \Delta\mathbf{T}_L \end{pmatrix} = \begin{pmatrix} \mathbf{G}_{sv} & \mathbf{0} \\ \gamma \cdot \mathbf{G}_{sh} & \mathbf{V}_{sv} \cdot \mathbf{G}_{sh} \end{pmatrix} \begin{pmatrix} \Delta\mathbf{V}_{sv} \\ \Delta\gamma \end{pmatrix}$$

More stable: spatial smoothing directly added

$$\left(\frac{V_{sh}+V_{sv}}{2}, \frac{2(V_{sh}-V_{sv})}{V_{sh}+V_{sv}}\right) \Leftrightarrow \left(V_{sv}\frac{\gamma+1}{2}, \frac{2(\gamma-1)}{\gamma+1}\right)$$

DRadiSurfTomo: application to SE Tibet

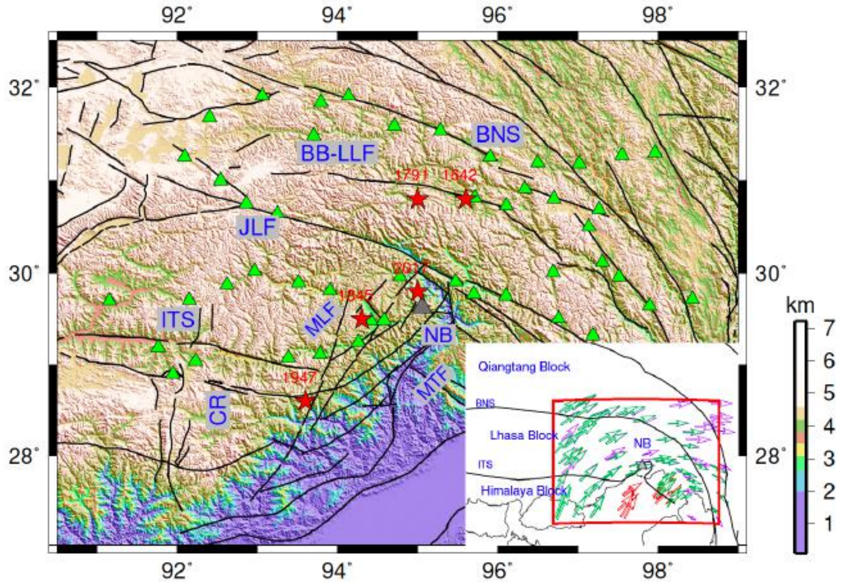

49 stations
ambient noise method
Vert. CFs → Rayleigh
Trans. CFs → Love

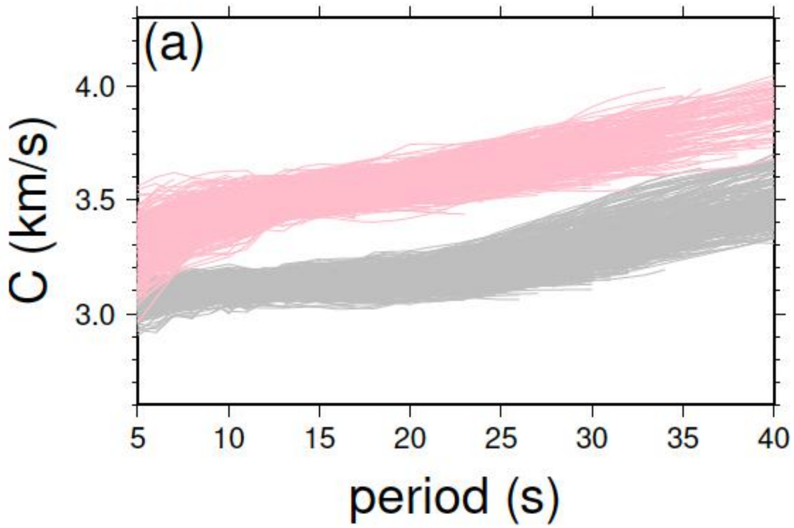

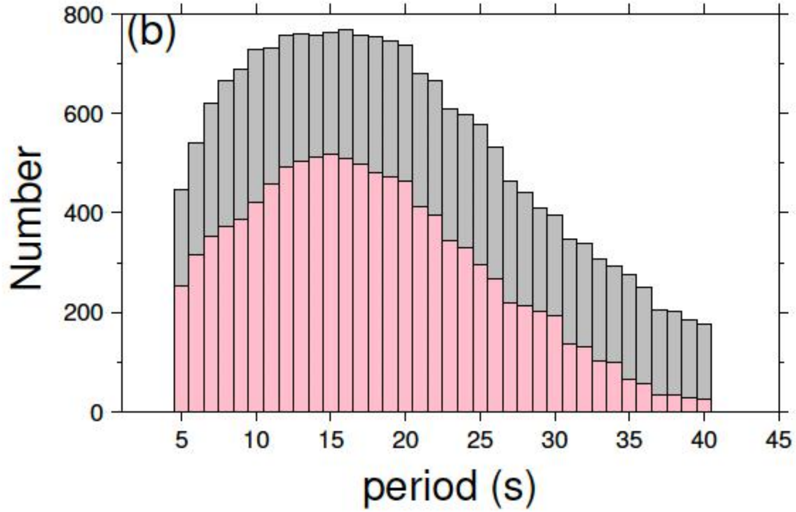

Synthetic examples: 3-D radial anisotropy

Direct division approach (ΔV_{sh}, ΔV_{sv})

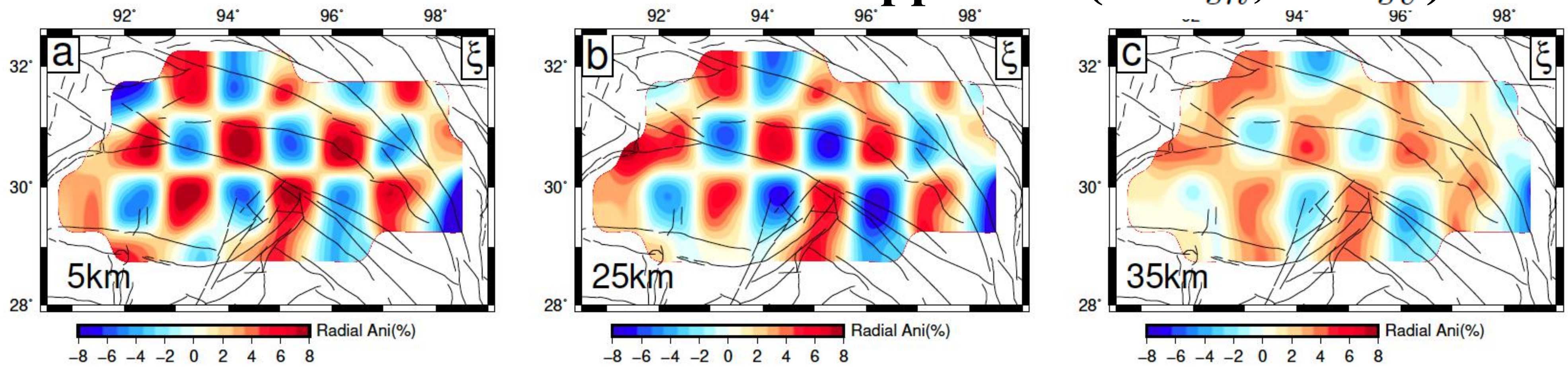

Direct inversion for radial aniso. (ΔV_{sv} , $\Delta\gamma$)

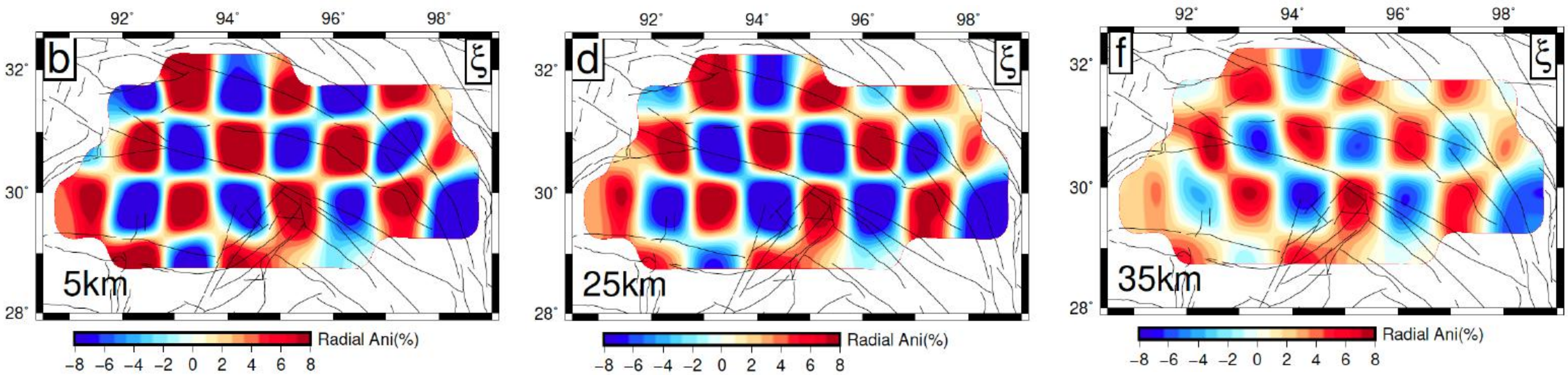

Hu, Yao, Huang (submitted to JGR)

3-D radial anisotropy in the upper and middle crust

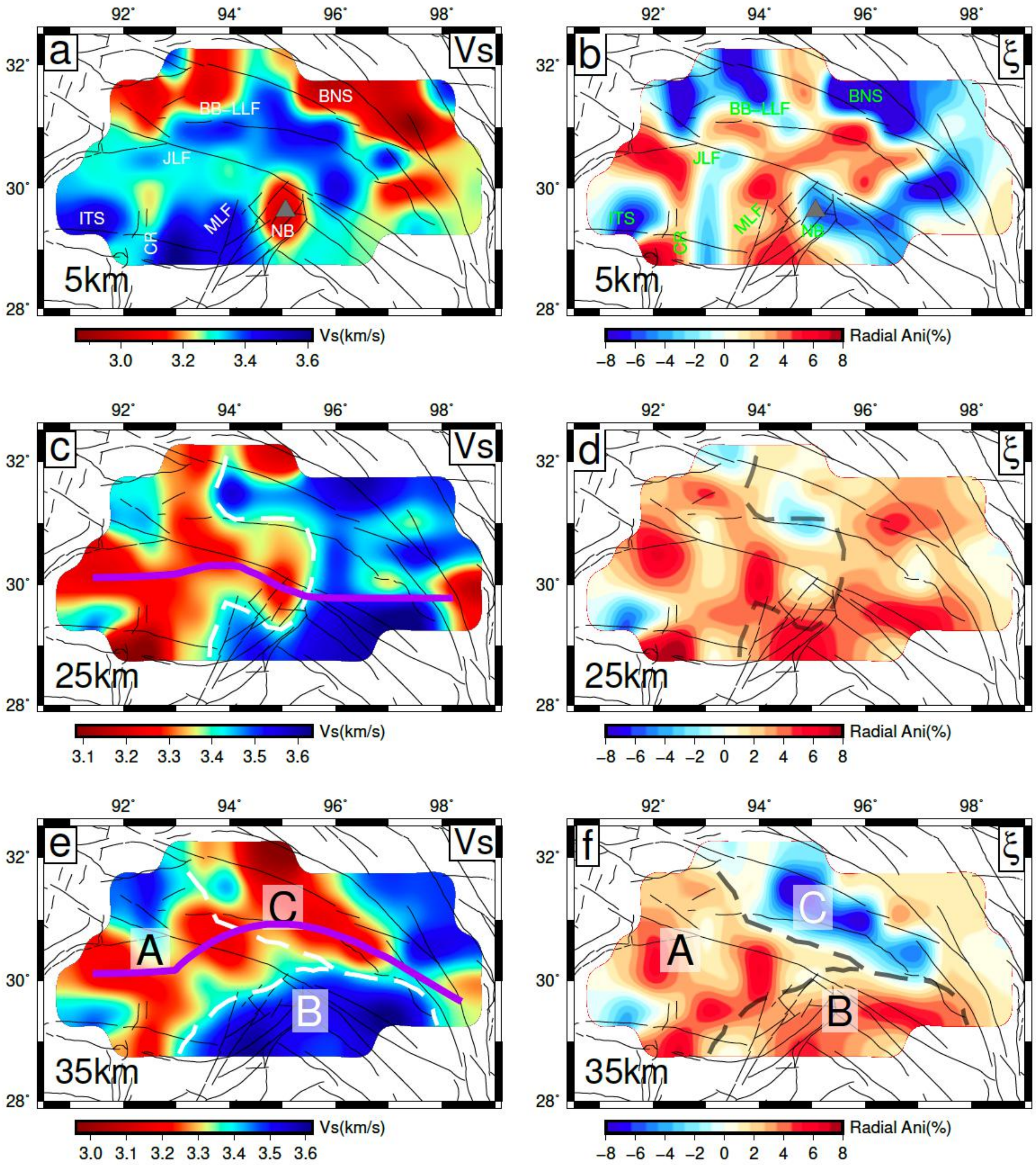

Hu, Yao, Huang (submitted to JGR)

Conclusions

1. Developed the joint inversion method of body & surface wave traveltime → more reliable 3-D Vp, Vs, and Vp/Vs models. Future work will include the station-based RFs and ZH data.
2. Developed direct inversion methods for 3-D azimuthal and radial anisotropy from surface wave traveltime data. Future work will include body wave traveltimes for 3-D joint anisotropy inversion.

Thank you!

hjyao@ustc.edu.cn
http://yaolab.ustc.edu.cn

DSurfTomo package download:
https://github.com/HongjianFang/DSurfTomo
DAzimSurfTomo package download:
https://github.com/Chuanming-Liu/DAzimSurfTomo
DBodySurfTomo & DRadiSurfTomo packages in progress